Decreased expression of a single tropomyosin isoform,TM5/TM30nm・results in reduction in motility of highly metastatic B16-F10 mouse melanoma cells

宮戸, 健二
九州大学医学系研究科分子生命科学系専攻

https://doi.org/10.11501/3123099

出版情報：九州大学, 1996, 博士（理学）, 課程博士
バージョン：
権利関係：

Decreased expression of a single tropomyosin isoform, TM5/TM30nm, results in reduction in motility of highly metastatic B16-F10 mouse melanoma cells

百戸俊二

(1)

Decreased expression of a single tropomyosin isoform, TM5/TM30nm, results in reduction in motility of highly metastatic B16-F10 mouse melanoma cells

by
Kenji Miyado

Contents

1. Summary

Tropomyosins are actin-binding proteins highly conserved in all eukaryotic cells with more than ten isoforms in non-muscle cells. However, the function and distribution of these proteins in non-muscle cells are not well understood. We directed our attention to one of tropomyosin isoforms, TM5/TM30nm, the expression of which was correlated with metastatic ability of several rodent cell lines.

We isolated a rat TM5/TM30nm cDNA clone, and prepared the polyclonal antibody against rat TM5/TM30nm C-terminal 16mer oligopeptide to examine the relation of this protein with malignant transformation of rat fibroblastic cells. We demonstaretd that expression of TM5/TM30nm RNA and this protein was higher in the tumorigenic rat fibroblastic cell lines SR-3Y1-2 and fos-SR-3Y1-202 cells than in the normal cell line 3Y1. In addition, the cellular localization of this protein differed between 3Y1 and tumorigenic ones.

In order to determine whether this elevated level of TM5/TM30nm plays a role in malignant phenotype, B16-F10 cells were transfected with recombinant DNA containing antisense rat TM5/TM30nm cDNA linked to the human metallothionein-IIa promoter, which is inducible by heavy metals such as zinc and cadmium. When the stably transfected clones were treated with $ZnSO_4$, decreased expression of TM5/TM30nm and reduction in cell motility, which is thought to be an indicator of cellular malignancy, were observed.

Furthermore, to identify a prototype of TM5/TM30nm, and/or a TM5/TM30nm related protein, immunoblotting of Saccharomyces cerevisiae cell extract was performed with anti-TM5/TM30nm antibody. A protein (45KDa) was recognized by this antibody, which showed slower mobility than hitherto known yeast TMs (23.5KDa and 33KDa). Using anti-TM5/TM30nm antibody, we isolated a cDNA clone from S.cerevisiae cDNA library. It encoded 317 amino acid residues. The putative sequence recognized by anti-TM30nm antibody was present in Asn-235 to Thr-250. The deduced amino acid sequence and hydropathy plot seggested that this protein has a tropomyosin-homologous sequence, transmembrane, and C-terminal basic regions.

2. Introduction

Cellular dynamics is largely maintained by an integrated action of cytoskeletal systems (1), which causes morphological changes, such as rounding up of cells (2) and the formation of membrane ruffling and extention of filopodia.

Recently, it has been shown that several growth factors induce alterations in the distribution of actin and actin-binding proteins. In particular, EGF is one of the most intensively studied polypeptide growth factors, and detailed knowledge has been obtained regarding the various effects on its target cells. These observation suggest that EGF causes changes in the organization of the cytoskeleton through a direct interaction between EGF receptor and actin-binding proteins. The candidates of such actin-binding proteins are fodrin (3), α-actinin (4), annexin (5), vinculin (6), which are components of the membrane-associated filament network. Those actin-binding proteins are co-immunoprecipitated with EGF receptor by anti-EGF receptor monoclonal antibody. The constitutive association of EGF receptor with the structural elements suggests that the interactions play a role in the regulation of cell motility. Association of EGF with its receptor causes activation of various kinases, resulting in a phosphorylation of several proteins including cytoskeletal proteins (7, 8), in addition to a phosphorylation of EGF receptor itself. The changes in phosphorylation state are thought to be involved in the association of EGF receptor with cytoskeletal elements and in signal transduction. In this respect, cytoskeletal systems have been suggested to play a role in signal transduction exerted by growth factors, relating to the initiation of DNA synthesis (9).

In addition, the function of cytoskeleton is known to be involved in protein sorting, the mechanism for transporting vesicles along microtubles and actin filaments within the cytoplasm (10). In contrast to the relative wealth of information concerning the sorting of membrane proteins, very little is understood about how cytosolic proteins are partitioned within the cytoplasm. However, it has become increasingly clear that the transport of mRNAs, and not the translated proteins themselves, constitutes an important way to localize cytosolic proteins. The first evidence for cytoplasmic mRNA localization came from the finding that actin transcripts are unevenly distributed in the ascidian embryo (11). More recently, localized mRNAs have been discovered in

somatic cells (12), indicating that mRNA localization serves as a general mechanism for creating asymmetric distributions of proteins in the cytoplasm. There should be an ordered pathway for mRNA localization. The recognition system to distinguish localized mRNAs from the majority of other RNAs has been just beginning to be deciphered. The cis-acting localization signals have been identified for a number of mRNAs, and all, without exception, lie within the 3'UTR (13, 14). Some element of the cytoskeleton is involved in anchoring messages, since localized mRNAs, in contrast to other mRNAs, are not solubilized by Triton X-100 (15). Actin filaments are the most likely candidates.

Actin is an abundant, highly conserved protein that is found in all eukaryotic cells. It is a major component of the cytoskeleton, and is involved in cell motility, mitosis and muscle contraction. Much has been learned about the polymerization of actin in vitro, including its regulation by small molecules (such as Ca2Å{and ATP) and actin-binding proteins (16, 17, 18).

Tropomyosins are actin-binding proteins with several isoforms, and numerous studies were directed to the relative abundance of tropomyosin isoforms in many cell types. Recent reports have noted that cytoskeletal isoforms are responsible for instability of stress fiber in several transformed cell lines. These studies suggest that tropomyosins may be associated with morphological changes that occur upon transformation (19). Rat tropomyosins are expressed from at least three genes, α-TM (20), β-TM (21), and TM-4 gene (22). The rat α-TM gene was shown to express more than seven transcripts by alternative splicing (20). In humans, a fourth gene termed hTMnm encoding TM30nm and TM30pl has been characterized in addition to the three genes equivalent to those found in rats (23). Presumably these genes evolved by duplication from a common ancestor (24). Clayton et al.(1988) revealed that this hTMnm gene family consists of a single structural gene independent of other tropomyosin families (23).

On the other hand, a human trk protooncogene, a fusion protein of cytoskeletal tropomyosin sequence to a putative tyrosine kinase is known (25). The region of tropomyosin in this protein is homologous to a human tropomyosin TM5/TM30nm. The viral oncogene, fgr, which includes actin

sequence also fused to a tyrosine kinase is similar to trk. Therefore, the relation of TM5/TM30nm to cellular transformation and/or malignant progression is an intriguing issue.

We isolated a rat TM5/TM30nm cDNA clone, and established anti-TM5/TM30nm antibody (RTM8-2) to assess the functional role of tropomyosin isoforms. We examined the expression of TM5/TM30nm in several cell lines including transformed cell lines and normal tissues. This protein was detecetd in almost all of nonmuscle cells and the expression was correlated with transformation and/or malignant progression in some cell lines. To further understand the function of TM5/TM30nm, we next directed our attention to TM5/TM30nm homologues in lower eukaryotes, in which the assay on the biological function of a molecule is relatively easy as compared with mammalian systems.

Yeast tropomyosin genes have been identified in S. cerevisiae (TPM1) (26), and Shizosaccharomyces pombe (cdc8) (27). The gene disruption experiments revealed that cdc8 has an essential role for growth, cell division or sporulation, while this was not the case of TPM1 in S. cerevisiae. Therefore, a second unidentified TM similar to cdc8 should be present in S. cerevisiae.

Thus, we tried to clone a TM5/TM30nm analogue in S. cerevisiae using RTM8-2 and several overlapping cDNA clones were isolated. The predicted product has tropomyosin-homologous sequence, antigen-like sequnce for anti-TM5/TM30nm antibody, a predicted trasmenbrane region and a C-terminal highly basic region. we named this product as **STRP** (S.cereviciae **T**M30nm **R**elated **P**rotein).

References

1. Ben-Ze'ev, A. (1985) The cytoskeleton of cancer cells. Biochem. Biophys. Acta. **780**, 197-212.
2. Chinkers, M., Mckanna, J. A. and Cohen, S. (1981) Rapid rounding of human epidermoid carcinoma cells A431 induced by epidermal growth factor. J. Cell Biol. **88**, 422-429.
3. Sobue, K., Kanda, K. and Kakiuchi, S. (1982) Solubilization and partial purification of protein kinase syetems from brain membarnes that phosphorylate calspectin. A spectrin-like calmodulin-binding protein (fodrin). FEBS Lett. **150**, 185-190.
4. Youssoufian, H., McAfee, M. and Kwiatkowski, D.J. (1990) Cloning and chromosomal localization of the human cytosleletal alpha-actinin gene reveals linkage to the beta-spacific gene. Am. J. Hum. Genet. **47**, 62-71.

5. Wice, B.M. and Gordon, J.I (1992) A strategy for isolation of cDNA encoding proteins affecting human intestinal epithelial cell growth and differentiation: Characterization of a novel gut-specific N-myristylated annexin. J. Cell Biol. **116**, 405-422.
6. Weller, P.A., Ogryzko, E.P., Corben, E.B., Zhidkova, N.E., Patel, B., price, G.J., Spurr, N. K., Koteliansky, V.E. and Critchley, D.R. (1990) Complete sequence of human vinculin and assignment of the gene to chromosome 10. Proc. Natl. Acad. Sci. U.S.A. **87**, 5667-5671.
7. Landreth, G.E., Williams, L.K. and Rieser, G.D. (1985) Association of the epidermal growth factor receptor kinase with the detergent-insoluble cytoskeleton of A431 cells. J. Cell Biol. **101**, 1341-1350.
8. Werth, D.K. and Postan, I (1984) Vinculin phosphorylation in response to calcium and phorbor esters in intact cells. J. Biol. Chem. **259**,5264-5270.
9. Thyberg, J. (1984) The microtubular cytoskeleton and the initiation of DNA synthesis. Exp. Cell Res. **155**, 1-8.
10. Schroer, T.A. (1992) Motors for fast axonal transport. Curr. Opin. Nerobiol. **2**, 618-621.
11. Jeffery, W.A., Tomlinson, C.R. and Brodeur, R.D. (1983) Localization of actin messenger RNA during early acidian development. Del. Biol. **99**, 408-417.
12. Singer, R.H. (1992) The cytoskeleton and mRNA localization. Curr. Opin. cell Biol. **4**, 15-19.
13. Mowry, K.L. and Melton, D.A. (1992) Vegetal messenger RNA localization directed by a 340-nt RNA sequence element in Xenopus oocytes. Science. **255**. 991-994.
14. Gottlieb, E. (1992) The 3' untranslated region of localized maternal messages contains a conserved motif involved in mRNA localization. Proc. Natl. Acad. Sci. U.S.A. **89**, 6174-6178.
15. Yisraeli, J.K., Sokol, S. and melton, D.A (1990) A two-step model for the localization of maternal mRNA in Xenopus oocytes: involvement of microtubules and microfilaments in the translocation and anchoring VgI mRNA. Development. **108**, 289-298.
16. Carlier, M.F. (1989) Role of nucleotide hydrolysis in the dynamics of actin filaments and microtubles. Int. Rev. Cytol. **115**, 139-170.
17. Pollard, T.D. and Cooper, J.A. (1986) Actin and actin-binding proteins. A critical evaluation of mechanisms and functions. Annu. Rev. Biochem. **55**, 987-1035.
18. Stossel, T.P., Chaponnier, C., Ezzell, R.M., Hartwig, J.H., Janmey, P.A., Kwiatkowski, D.J., Lind, S.E., Smith, D.B., Southwick, F.S. and Yin, H.L. (1985) Nonmuscle actin-binding proteins. Annu. Rev. Cell Biol. **1**, 353-402.
19. Matsumura, F., Lin, J., Yamashiro-Matsumura, S., Thomas, G.P. and Topp, W.C. (1983) Differential expression of tropomyosin isoforms in the microfilaments isolated from normal and transformed rat cultured cells. J. Biochem. Chem. **258**, 13954-13964.
20. Goodwin, L.O., Lees-Miller, J.P., Leonard, M.A., Cheley, S.B. and Helfman, D.M. (1991) Four fibroblast tropomyosin isoforms are expressed from the rat Éø-tropomyosin gene via alternative RNA splicing and the use of two promoters. J. Biol. Chem. **266**, 8408-8415.

21. Helfman, D.M., Cheley, S., Kuismanen, E., Finn, L.A. and Yamawaki-Kataoka, Y. (1986) Nonmuscle and muscle tropomyosin isoforms are expressed from a single gene by alternative RNA splicing and polyadenylation. Mol. cell. Biol. **6**, 3582-3595.

22. Lees-Miller, J.P., Yan, A. and Helfman, D.M. (1990) Structure and complete nucleotide sequence of the gene encoding rat fibroblast tropomyosin 4. J. Mol. Biol. **213**, 399-405.

23. Clayton, L., Reinach, F.C., Chumbley, G.M. and MacLeod, A.R. (1988) Organization of the hTMnm gene: Implications for evolution of muscle and non-muscle tropomyosins. J. Mol. Biol. **201**, 507-515.

24. Lees-Miller, J.P. and Helfman, D.M. (1991) The molecular basis for tropomyosin isoform diversity. Bioessays **13**, 429-437.

25. Martin-Zanca, D., Hughes, S.H. and Barbacid, M. (1986) A human oncogene formed by the fusion of truncated tropomyosin and protein tyrosine kinase sequences. Nature. **319**, 743-748.

26. Liu, H. and Bretsher, A. (1989) Disruption of the single tropomyosin gene in yeast results in the disappearance of actin cables from the cytoskeleton. Cell. **57**, 233-242.

27. Balasubramanian, M.K., Helfman, D.M. and Hemmingsen, S.M. (1992) A new tropomyosin essential for cytokinesis in the fission yeast S. pombe. Nature **360**, 84-87.

Transformation-related expression of a low-molecular weight tropomyosin isoform TM5/TM30nm in transformed rat fibroblastic cell lines

Abstract We cloned a full-length rat TM5/TM30nm cDNA. Using this cDNA as a probe, we demonstrated that expression of TM5/TM30nm mRNA was higher in the tumorigenic rat fibroblastic cell lines SR-3Y1-2 and fos-SR-3Y1-202 than in the normal cell line 3Y1. High expression of TM5/TM30nm protein in SR-3Y1-2 and fos-SR-3Y1-202 cells was also detected by Western blot analysis using anti-TM5/TM30nm antiserum. In addition, the cellular localization of this protein differed between 3Y1 cells and tumorigenic ones. These findings suggest that TM5/TM30nm is involved in malignant transformation of rat fibroblastic cells.

Introduction

Tropomyosins (TMs) are actin-associated cytoskeletal proteins of muscle and non-muscle cells. Multiple isoforms of TMs are found in vertebrate non-muscle cells (28, 29, 30). There are at least seven TM isoforms expressed in non-muscle cells: three high-molecular weight TMs, TM1, TM2 and TM3, and four low-molecular weight TMs, TM4, TM5a, TM5b and TM30nm (also termed TM5 for mouse; hereinafter referred to as TM5/TM30nm).

In mammals, a number of studies have shown that the synthesis of certain TMs, particularly the isoforms of apparently high-molecular weight TMs, is suppressed when cultured cells exhibit neoplastic transformed phenotype induced by various retroviral oncogenes (31, 32, 33, 34), carcinogens (35), or growth factors (34). In addition, transfection of TMs including TM1 and TM2 into viral oncogene-transformed rodent cells suppresses tumorigenic phenotypes (36, 37). These observations suggest that isoform-specific regulation of TM synthesis is related to the microfilament aberrations observed in diverse types of tumor cells (30).

Recently, we found that expression of TM5/TM30nm, a low-molecular- weight TM isoform, was higher in a high-metastatic B16 mouse cell line, B16-F10, than in a low-metastatic mouse cell line, B16-F1 (38). Moreover, this elevated expression of TM5/TM30nm could be suppressed by the expression of antisense TM5/TM30nm cDNA, and reduction of expression of TM5/TM30nm was well correlated with decrease in cell motility, one of the indicators of metastatic activity (38).

In this study, we extended our previous study in an attempt to determine whether elevated synthesis of TM5/TM30nm is also associated with malignant transformation.

Materials and methods

Cell culture The cell lines used were 3Y1, SR-3Y1-2 and fos-SR-3Y1-202. SR-3Y1-2 is a clonal cell line derived from a normal rat fibroblastic cell line, 3Y1 (39), by transfection with Rous sarcoma virus (40). The fos-SR-3Y1-202 cell line is a clonal cell line that was established by transfection of the parent cell line, SR-3Y1-2, with a proviral v-fos-containing plasmid DNA (40). Cells were grown at 37°C in Dulbecco's modified Eagle's medium (DMEM; GIBCO BRL, Gaithersburg, MD) supplemented with 10% fetal bovine serum (FBS) and bicarbonate (3.7 g/liter) in a moist atmosphere of 10% CO_2 and 90% air. Cells at subconfluency were harvested and subjected to Northern and Western blot analyses.

Cloning of rat TM5/TM30nm cDNA To isolate a rat TM5/TM30nm cDNA clone, a rat cDNA library derived from rat hepatoma NH (41) was screened using a probe for a 0.8-kilobase pairs (kb) 3'-untranslated region (3'-UTR) of mouse TM5 cDNA (42), which was kindly provided by Dr. S. Sakiyama (Chiba Cancer Center, Chiba, Japan). We obtained 4 clones that positively hybridized with the probe. Of these four, one clone (termed clone #8) had the longest insert for rat TM5/TM30nm cDNA, but lacked a 5' portion, including the ATG codon, possessed by mouse TM5 cDNA (42). When re-screening was performed with a rat macrophage cDNA library (Clontech, Palo Alto, CA) using the insert excised from clone #8 as a probe, we finally obtained a full-length cDNA clone (termed clone #11) for TM5/TM30nm. The EcoRI-digested cDNA insert was then subcloned into pSP65 (43), and characterized by restriction-endonuclease mapping and sequencing.

Preparation of antiserum Anti-TM5/TM30nm antiserum, termed RTM8-2 (44), was prepared by immunizing rabbits with an oligopeptide (^{233}CTQRMLDQT LLDLNEM^{248}) corresponding to the C-terminal region of rat TM5/TM30nm; this region is completely conserved among man, rat and mouse (42, 45).

Western blot analysis Proteins (20 μg per lane) were electrophoresed and immunoblotted onto nitrocellulose filters (S&S GmbH, Dassel, Germany) that had been immersed in RTM8-2 (diluted 1: 500), as described previously (46). Positive signals were quantitated using a densitometer (DH303, Advantec, CA). In some cases, anti-actin antiserum (Amersham, Buckinghamshire, England) was used as a control.

Northern blot analysis Total RNA was isolated by the guanidium isothiocyanate method (47). RNA (20 μg/lane) was electrophoresed on a 1.5% agarose/formaldehyde gel and blotted onto a nitrocellulose filter (S&S GmbH). RNA blotting was performed as previously described (47). The filter membrane was then hybridized with an α[^{32}P]-dCTP-labeled rat TM5/TM30nm cDNA. The same filter was also hybridized with human β-actin gene after dehybridization. Positive hybridization signals on X- ray film were quantitated using the densitometer.

Immunohistochemical analysis Cells on glass coverslips at subconfluency were fixed in 4% paraformaldehyde in phosphate-buffered saline, pH 7.2 (PBS) for 10 min and permeabilized by treatment with 1% Triton X-100 containing 10 mM Tris-HCl, pH 7.9, 30 mM KCl, 10 mM $MgCl_2$ and 10 mM 2-mercaptoethanol for 1 min at room temperature, and then fixed in ice-cold methanol for 20 min at room temperature. After air-drying, remaining cytoskeletons or whole cells on coverslips were incubated with RTM8-2 [first antiserum; diluted 1/500 in PBS+0.1% bovine serum albumin (BSA)] for 1 h at 4°C. After washing with PBS+0.1% BSA, they were then incubated with rhodamine-conjugated goat anti-rabbit IgG (second antibody; MBL, Nagoya, Japan) for 1 h at room temperature. As a control, specimens were incubated with the second antibody following incubation with PBS+0.1% BSA instead of the first antiserum.

Results

Rat TM5/TM30nm cDNA and the predicted amino acid sequence

The longest cDNA isolated from the rat macrophage cDNA library was 1.77 kb in size and contained 65 and 970 bp nucleotide (ntd) 5' and 3' untranslated regions, respectively (Fig.1). During the cloning, a report of the isolation of rat TM5/TM30nm cDNA (termed rTMnmNM-1) (48) became available. The deduced amino acid sequence of our rat TM5/TM30nm cDNA completely matched that of rTMnmNM-1, except for one amino acid residue (83rd amino acid), i.e., Val (GTT) in rat TM5/TM30nm and Ala (GCT) in rTMnmNM-1. The predicted open reading frame encodes 248 amino acids, 2 positions (fourth and 83rd) of the amino acid sequence of which differed among species: for the fourth amino acid, Ser (AGC) in rats, Thr (ACC) in mice and Ile (ATC) in humans, and for 83rd amino acid, Val (GTT) in the rats we used and Ala (GCT) in mice and humans (42, 45, 48). Harrplot analysis revealed high degrees of similarity (76.0 and 92.9%, respectively) between human and mouse counterparts at the nucleic acid level, as expected. A slight difference at a nucleic acid level in the coding region between TM5/TM30nm and rTMnmNM-1 cDNAs may have been due to the difference in rat strains used.

Difference in TM5/TM30nm mRNA expression between 3Y1 and transformed 3Y1 cell lines

As previously noted (39), SR-3Y1-2 cells were derived from 3Y1 cells by transfection with Rous sarcoma virus. The fos-SR-3Y1-202 cell line was constructed by transfection of SR-3Y1-2 cells with the proviral v-fos-containing plasmid. In contrast to 3Y1 cells, which exhibit contact-inhibition upon confluency and have a relatively flat shape, both SR-3Y1-2 and fos-SR-3Y1-202 cells were round in shape (Fig. 2A) and did not exhibit contact inhibition even after achieving confluency. Image analysis measurements indicated that fos-SR-3Y1-202 cells have a motility index ca. 2.3 times higher than that of SR-3Y1-2 cells (49), suggesting that fos-SR-3Y1-202 cells are more metastatic than SR-3Y1-2 cells, since motility is a critical requirement for tumor cell invasion and metastasis (50, 51, 52). Furthermore, in the experimental metastasis by *i.v.* inoculation of cells into rats, the fos-SR-3Y1-202 cells produced more colonies on the lung than did SR-3Y1-2 cells (40). Thus, it is suggested that metastatic activity is in the following order: fos-SR-3Y1-202> SR-3Y1-2> 3Y1.

Using the 1.77-kb rat TM5/TM30nm cDNA as a probe, we examined the expression of rat TM5/TM30nm mRNA in three fibroblastic cell lines (3Y1, SR-3Y1-2 and fos-SR-3Y1-202) by Northern blot analysis. The results are shown in Fig. 2B. Expression of TM5/TM30nm mRNA (which is detected at a size of ca. 2,000 ntds) was observed in all of these cell lines. Notably, expression of TM5/TM30nm mRNA was 2.43 and 11.00-fold increased in the high-metastatic lines SR-3Y1-2 and fos-SR-3Y1-202, respectively, compared to that of the low-metastatic parental cell line 3Y1. Furthermore, the fos-SR-3Y1-202 cells expressed 2-fold higher amounts of transcripts than the SR-3Y1-2 cells. These findings suggest that a close correlation exists between the degree of expression of TM5/TM30nm mRNA and that of malignancy of SR-3Y1-2 and fos-SR-3Y1-202 cells.

Western blot analysis by TM5/TM30nm antiserum

To determine whether the two oncovirally transformed rat fibroblastic cell lines SR-3Y1-2 and fos-SR-3Y1-202 exhibit increased levels of TM5/TM30nm protein, cellular proteins were subjected to one-dimensional polyacrylamide gel electrophoresis and then transferred to filters for Western blot analysis using RTM8-2 (Fig. 3, light column). As expected, the levels of TM5/TM30nm protein

(which are indicated as a band at a molecular weight of 31 kDa) were 1.45 and 1.52-fold increased in SR-3Y1-2 and fos-SR-3Y1-202, respectively, compared to that in the parental 3Y1 cells. This size is consistent with the previous finding that human TM30nm mRNA encoded an approximately 30-kDa molecular weight polypeptide, when translation products of TM30nm mRNA in a cell-free system were analyzed by two-dimensional gel electrophoresis (45). The band at a molecular weight of 32.5 kDa, which featured a higher molecular weight than the 31-kDa TM5/TM30nm protein, was also reactive with RTM8-2, particularly for SR-3Y1-2 and fos-SR-3Y1-202 (Fig. 3, light column). Since the 32.5-kDa protein observed in SR-3Y1-2 and fos-SR-3Y1-202 cells was not found in any normal non-musclar organs including brain, bone marrow, lung, kidney, liver and spleen or in musclar organs including heart (data not shown), it is possible that the 32.5-kDa protein recognized by RTM8-2 is associated with tumorigenesis. It would be of interest to determine whether the 32.5-kDa protein is highly expressed in other transformed cell lines and whether its function is similar to that of TM5/TM30nm. In contrast, the quantity of actin protein was the same in all of the cell lines examined (Fig. 3, left column).

Immunohistochemical analysis of 3Y1 and transformed 3Y1 cell lines

To determine the cellular localization of TM5/TM30nm protein in SR-3Y1-2 and 3Y1 cells, an immunohistochemical study was performed using RTM8-2 (Fig. 4). In the low-metastatic 3Y1 cells, well-defined bundles of actin microfilaments (stress fibers) reactive with the antiserum were evident throughout the cytoplasm (Fig. 4A). On the other hand, in the tumorigenic SR-3Y1-2 cells, the RTM8-2-reactive stress fibers were reduced in number and integrity; many cells lacked them entirely, and instead exhibited dot-like structures throughout the cytoplasm (Fig. 4B). In the fos-SR-3Y1-202 cells, the localization of TM5/TM30nm was similar to that in SR-3Y1-2 cells (data not shown). In the control (incubation without the first antiserum), no staining was observed for either 3Y1 or SR-3Y1-2 cells (data not shown). When double staining using anti-actin and anti-TM5/TM30nm antibodies was carried out for SR-3Y1-2 cells, the RTM8-2-reactive areas were also stained by anti-actin antibody (data not shown). While stress fibers were clearly and highly formed in 3Y1, we observed the disintegrity of stress fibers in SR-3Y1-2 cells. These findings suggest

that i) TM5/TM30nm is associated with cytoplasmic microfilaments, and ii) overexpression of TM5/TM30nm inhibits the polymerization and/or the formation of the bundles of actin microfilaments.

Discussion

In this study, we demonstrated using rat TM5/TM30nm cDNA as a probe and an anti-rat TM5/TM30nm antiserum, RTM8-2, that expression of TM5/TM30nm was higher in tumorigenic, oncovirally transformed rat fibroblastic cells than in normal parental cells at both the mRNA and protein levels.

Numerous studies have provided evidence that high-molecular weight TM isoforms are involved in the malignant transformation of cells; the levels of high-molceular weight TM isoforms are reduced in cells transformed by oncoviral or chemical reagents, and increased when the cells have reverted to normal (34, 53). These findings suggest that these high-molecular weight TM isoforms probably play a role in microfilament organization through polymerization of actin molecules. In this study, we demonstrated that expression of the TM5/TM30nm molecule is increased in association with oncovirus-mediated transformation of rat fibroblastic cells. More interestingly, the expression of this molecule appears to be correlated with metastasis, since the high-metastatic line fos-SR-3Y1-202 exhibited higher expression of TM5/TM30nm than did SR-3Y1-2 (see Figs. 2B, 3). Similar findings were also obtained for the high-metastatic mouse melanoma cell line B16-F10 and the low-metastatic cell line B16-F1 (38). In the present study, immunohistochemical experiments using RTM8-2 revealed that well-defined bundles of microfilaments were present in normal parental 3Y1 cells, but not in the transformed cell line, SR-3Y1-2 (see Fig. 4). Since it has shown that the levels of TM5 are increased upon transformation by either DNA or RNA viruses (32), these findings suggest that TM5/TM30nm is involved in the transformation of several types of tumor cells, probably by enhancing depolymerization of microfilaments. The low- and high-molecular weight TM isoforms appear to be functionally different. This may be explained by the facts that i) the amino-terminal region is highly conserved

among muscle and high-molecular weight TMs, but not among low-molecular weight TMs (45), and ii) deletion of the amino-terminal region (residues 1-9) of muscle TM isoforms resulted in loss of actin-binding ability, indicating the importance of the amino-terminus sequence for the interaction with actin molecule (54). Since it has been reported that expression of TM5/TM30nm is unchanged in certain tumor cell lines (55), the present finding that increased expression of TM5/TM30nm occurs in association with malignancy suggests that expression of TM5/TM30nm depends upon the cell type examined.

In summary, we found that increased synthesis of TM5/TM30nm occurred in transformed rat fibroblastic cells. These findings will be useful for analysis of the etiology of malignancy and for development of antisense oligonucleotides for the TM5/TM30nm gene as an anti-tumor therapeutic reagent.

References

28. Cote, G.P. (1983) Structural and functional properties of the non-muscle tropomyosins. Mol. Cell. Biochem. **57**,127-146.
29. Lin, J.J.C., Helfman, D.M., Hughes, S.H. and Chou, C.S. (1985) Tropomyosin isoforms in chicken embryo fibroblasts: purification, characterization and changes in Rous sarcoma virus-transformed cells. J. Cell Biol. **100**, 692-703.
30. Matsumura, F. and Yamashiro-Matsumura, S. (1985) Purification and characterization of multiple isoforms of tropomyosin from rat cultured cells. J. Biol. Chem. **260**, 13851-13859.
31. Leonardi, C.L., Warren, R.H. and Rubin, R.W. (1982) Lack of tropomyosin correlates with the absence of stress fibers in transformed rat kidney cells. Biochem. Biophys. Acta **720**, 154-162.
32. Matsumura, F., Lin, J.J.C., Yamashiro-Matsumura, S., Thomas, G.P. and Topp, W.C. (1983) Differential expression of tropomyosin forms in the microfilaments isolated from normal and transformed rat cultured cells. J. Biol. Chem. **258**, 13954-13964.
33. Hendricks, M. and Weintraub, H. (1984) Multiple tropomyosin polypeptides in chicken embryo fibroblasts: differential repression of transcription by Rous sarcoma virus transformation. Mol. Cell. Biol. **4**, 1823-1833.
34. Cooper, H.L., Bhattacharya, B., Bassin, R.H. and Salomon, D.S. (1987) Suppression of synthesis and utilization of tropomyosin in mouse and rat fibroblasts by transforming growth factor-alpha: a pathway in oncogene action. Cancer Res. **47**, 4493-4500.

35. Leavitt, J., Latter, G., Lutomski, L., Goldstein, D. and Burbeck, S. (1986) Tropomyosin isoform switching in tumorigenic human fibroblasts. Mol. Cell. Biol. **6**, 2721-2726.
36. Prasad, G.L., Fuldner, R.A. and Cooper, H.L. (1993) Expression of transduced tropomyosin 1 cDNA suppresses neoplastic growth of cells transformed by the ras oncogene. Proc. Natl. Acad. Sci. USA **90**, 7039-7043.
37. Takenaga, K. and Masuda, A. (1994) Restoration of microfilament bundle organization in v-raf-transformed NRK cells after transduction with tropomyosin 2 cDNA. Cancer Letters **87**, 47-53.
38. Miyado, K., Kimura, M. and Taniguchi, S. (1996) Decreased expression of a single tropomyosin TM5/TM30nm results in reduction in motility of highly metastatic mouse melanoma cell line B16-F10. Biochem. Biophys. Res. Commun. **225**, 427-435.
39. Kimura, G., Itagaki, A. and Summers, J. (1975) Rat cell line 3Y1 and its virogenic polyoma- and SV40-transformed derivatives. Int. J. Cancer **15**, 694-706.
40. Taniguchi, S., Kawano, T., Mitsudomi, T., Kimura, G. and Baba, T. (1986) Fos oncogene transfer to a transformed rat fibroblast cell line enhances spontaneous lung metastasis in rats. Jpn. J. Cancer Res. **77**, 1193-1197.
41. Nishikawa, K. and Baba, T. (1981) Special combination of anticancer drug with its antidote for chemotharapy of liver metastasis. Gan to Kagakuryoho **8**, 180-186.
42. Takenaga, K., Nakamura, Y., Kageyama, H. and Sakiyama, S. (1990) Nucleotide sequence of cDNA for nonmuscle tropomyosin 5 of mouse fibroblast. Biochem. Biophys. Acta **1087**, 101-103.
43. Melton, D.A., Krieg, P.A., Rebagliati, M.R., Maniatis, T., Zinn, K. and Green, M.R. (1984) Efficient in vitro synthesis of biologically active RNA and RNA hybridization probes from plasmids containing a bacteriophage SP6 promoter. Nucleic Acids Res. **12**, 7035-7056.
44. Miyado, K., Katsuki, M. and Taniguchi, S. (1994) Isolation of a yeast tropomyosin-related cDNA clone that encodes a novel transmembrane protein having a C-terminal highly basic region. Biochem. Biophys. Res. Commun. **199**, 1363-1371.
45. MacLeod, A.R., Houlker, C., Reinach, F.C. and Talbot, K. (1986) The mRNA and RNA-copy pseudogenes encoding TM30nm, a human cytoskeletal tropomyosin. Nucleic Acid Res. **14**, 8413-8426.
46. Okamoto-Inoue, M., Taniguchi, S., Sadano, H., Kawano, T., Kimura, G., Gabbiani, G. and Baba, T. (1990) Alteration in expression of smooth muscle α-actin associated with transformation of rat 3Y1 cells. J. Cell Sci. **96**, 631-637.
47. Sambrook, J., Fritsch, E.F. and Maniatis, T. (1989) Molecular Cloning: A Laboratory Mannual, 2nd edn. Cold Spring Harbor Laboratory, Cold Spring Harbor, NY
48. Beisel, K.W., Kennedy, J.E. (1994) Identification of novel alternatively spliced isoforms of the tropomyosin-encoding gene, *TMnm*, in the rat cochlea. Gene **143**, 251-256.

49. Taniguchi, S., Tatsuka, M., Nakamatsu, K., Sadano, H., Okazaki, H., Iwamoto, H. and Baba, T. (1989) High invasiveness associated with augmentation of motility in a fos-transferred highly metastatic rat 3Y1 cell line. Cancer Res **49**, 6738-6744.

50. Volk, T., Geiger, B. and Raz, A. (1984) Motility and adhesive properties of high-and low-metastatic murine neoplastic cells. Cancer Res. **44**, 811-814.

51. Liotta, L.A., Mandler, R., Murano, G., Katz, D.A., Gordon, R.K., Chiang, D.K. and Schiffmann, E. (1986) Tumor cell autocrine motility factor. Proc. Natl. Acad. Sci. USA **83**, 3302-3306.

52. Mohler, J.L., Partin, A.W., Isaacs, J.T. and Coffey, D.S. (1988) Metastatic potential prediction by a visual grading system of cell motility: prospective variation in the dunning R-3327 prostatic adenocarcinoma nodules. Cancer Res. **48**, 4312-4317.

53. Cooper, H.L., Feuerstein, N., Noda, M. and Bassin, R.H. (1985) Suppression of tropomyosin synthesis, a common biochemical feature of oncogenesis by structurally diverse retroviral oncogenes. Mol. Cell. Biol. **5**, 972-983.

54. Cho, Y.-J., Liu, J.L. and Hitchcock-DeGregori S.E. (1990) The amino terminus of muscle tropomyosin is a major determinant for function. J. Biol. Chem. **265**, 538-545.

55. Novy, R.E., Lin, J.L., Lin, C.S. and Lin, J.J. (1993) Human fibroblast tropomyosin isoforms: characterization of cDNA clones and analysis of tropomyosin isoform expression in human tissues and in normal and transformed cells. Cell. Motil. Cytoskeleton **25**, 267-281.

Figure legends

Fig. 1 Rat TM5/TM30nm cDNA and predicted amino acid sequence.
This cDNA was 1.77-kb in size and contained 65 and 970 bp ntd 5' and 3' untranslated regions, respectively.

```
   1 GCTACAACGCCGAGCGGAGGAGGTAGGAACCTGATTTCCAGAAGCAGCTGGGTAGGCACCATGGCCGGGAGCACCACCATCGAGGCGGTA
                                                                M  A  G  S  T  T  I  E  A  V  10
  91 AAGCGCAAGATCCAGGTTCTGCAGCAGCAGGCTGATGTGCAGGAGGAGAGGGCCGAGCGCCTCCAGCGGGAAGTGGAGGGAGAAAGGCGG
      K  R  K  I  Q  V  L  Q  Q  Q  A  D  D  A  E  E  R  A  E  R  L  Q  R  E  V  E  G  E  R  R  40
 181 GCCCGGGAGCAGGCTGAAGCTGAGGTGGCCTCCTTGAACCGCAGGATCCAGCTGGTTGAAGAGGAGCTGGACCGCGCCCAGGAGCGCCTT
      A  R  E  Q  A  E  A  E  V  A  S  L  N  R  R  I  Q  L  V  E  E  E  L  D  R  A  Q  E  R  L  70
 271 GCCACTGCTTTGCAGAAGCTGGAGGAAGCAGAGAAGGTTGCTGATGAGAGTGAGAGAGGTATGAAGGTGATTGAAAACCGGGCTCTAAAA
      A  T  A  L  Q  K  L  E  E  A  E  K  A  A  D  E  S  E  R  G  M  K  V  I  E  N  R  A  L  K  100
 361 GATGAAGAAAAGATGGAGCTCCAGGAAATCCAGCTGAAGGAAGCAAAGCACATTGCAGAAGAGGCAGACAGGAAGTATGAAGAGGTGGCT
      D  E  E  K  M  E  L  Q  E  I  Q  L  K  E  A  K  H  I  A  E  E  A  D  R  K  Y  E  E  V  A  130
 451 CGTAAGTTGGTGATTATTGAAGGAGACTTGGAACGCACGGAGGAACGCGCCGAGCTGGCAGAGTCCCGTTGCCGAGAGATGGATGAGCAG
      R  K  L  V  I  I  E  G  D  L  E  R  T  E  E  R  A  E  L  A  E  S  R  C  R  E  M  D  E  Q  160
 541 ATCAGACTGATGGACCAGAACCTGAAGTGTCTGAGTGCTGCTGAAGAAAAGTACTCTCAAAAAGAAGACAAGTATGAAGAAGAAATAAAG
      I  R  L  M  D  Q  N  L  K  C  L  S  A  A  E  E  K  Y  S  Q  K  E  D  K  Y  E  E  E  I  K  190
 631 ATTCTTACTGATAAACTCAAGGAGGCGGAGACCCGGGCTGAGTTTGCTGAAAGATCGGTAGCCAAACTGGAAAAGACCATTGATGACTTG
      I  L  T  D  K  L  K  E  A  E  T  R  A  E  F  A  E  R  S  V  A  K  L  E  K  T  I  D  D  L  220
 721 GAAGATAAGCTGAAGTGCACCAAAGAGGAGCATCTCTGTACACAAAGGATGCTGGACCAGACCCTGCTGGACCTGAACGAGATGTAGACC
      E  D  K  L  K  C  T  K  E  E  H  L  C  T  Q  R  M  L  D  Q  T  L  L  D  L  N  E  M        248
 811 TTCCCCATCCCTGCCCTGCCCTGCGGCCGCTCCTCCCTCTGACCTTGACTCCGCCTGAGGCCAGCCTCCCTGAAGCTGGCTTGAAACTGA
 901 GGGCTGATCTTTTTAACTGAAGGCTGCTTTCCCTCCTGCCACCCCTCTTACCCCTCTTGTCTTTTTCATCAAAACTGTGTCAGCCTCTTC
 991 CCAGAGTTCCAGCTGGAGGGTCTGAACACTCTTTGGGAATCAATATTTAAGGGAATGTGAGCACAGCGCAAAGTGTCCTCAATGCAGTTG
1081 TGATATGCACATTGTGATTACTTTTTGTCTTAGCAACCATTTTAACATTCCAAGCACTTGGCAGCTTGGTGCAGCACATCTTAGCCTAAT
1171 GGATACCGTCTCTCCATGGAGGAGAAACACAGGAATGGGCCTGCTTACTGAGAGCCAGCAGAGCCCAGGCAGACTCCACTGTGGAGACCT
1261 CAGTGCTCTGTACCAAGTCTTAGCCAAACAACAGGGTTCTAGGAAGTTAGCCAAAAACAAAAACCATTCCGGTCTGTGAAGGAAAACAGC
1351 TTTGATATCTTTGAACAACTTTACACTTATTTTTAGTTTTGACTTTTTCCGTCCGATGTGACCAAATAGGAGAGTGAGACATCTGAGACG
1441 CCCCCGCCTCCCAGGGCCCTTGTGCATGTTAGGCCAGCGTGCTACCGTTCACCCCCAGCCCTGAGCCCGAACTTGTCTCAGCTCTACCCC
1531 TTTCCCAACTGCTCAGAAATGGATCATGCTGCCCCTTAGTGTTGTGGTGACCTCTTAGTGTTCACCTGCCCCAAGGGAGACGGAAAAGGA
1621 AATTATGTTTGTGCCACTGATTTAGCCACATGAAAGTCATCTCATTGCTCTTTCCTGAAGCTGCTGTCTCTAAAGTGCCATCTCTTTGTG
1711 CTTTGTATCAGTCAGTGCTGGAGAAATCTTGAATAGCTTATGTTTAAAAAAAAAAAAAAA
```

Fig. 2 Microphotographs of rat fibroblastic cell lines (3Y1, SR-3Y1-2 and fos-SR-3Y1-202) and Northern blot analysis using rat TM5/TM30nm cDNA as a probe. **A**, inverted microscopic observation. 3Y1 cells retain contact-inhibition of growth and exhibit flat shape, but oncovirally tranformed cells (SR-3Y1-2 and fos-SR-3Y1-202) are round and have lost contact-inhibition of growth. Note that the fos-SR-3Y1-202 cells are rounder than the SR-3Y1-2 cells, suggesting that the former cells are more metastatic than the latter (see text). The bars indicate 100 μm. **B**, mRNA expression in rat fibroblastic cell lines 3Y1, SR-3Y1-2 and fos-SR-3Y1-202. In all the cells examined, a single band with ca. 2,000 ntds was detected when RNAs were probed with labeled rat TM5/TM30nm cDNA (upper column). Note that expression of TM5/TM30nm mRNA is increased in SR-3Y1-2 and fos-SR-3Y1-202 cells compared with that in the parental 3Y1 cell line. The lower column shows the pattern of hybridization with β-actin probe, and reveals no significant difference in the level of β-actin mRNA among the cell lines. Molecular weight markers of 28S and 18S ribosomal RNAs are shown on the left side.

A

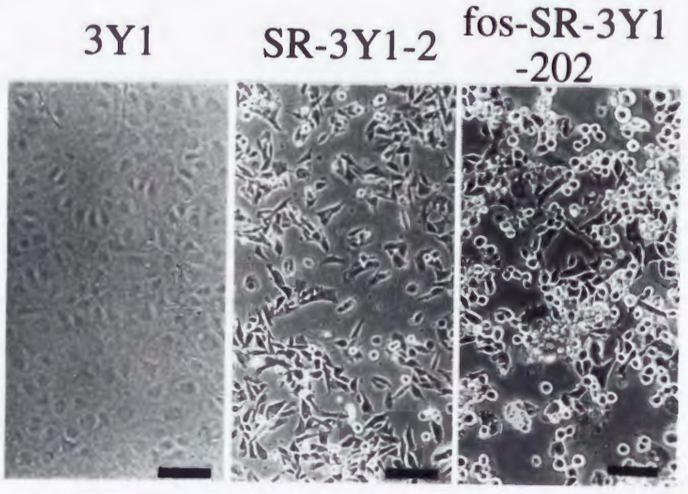
3Y1
SR-3Y1-2
fos-SR-3Y1
-202

B

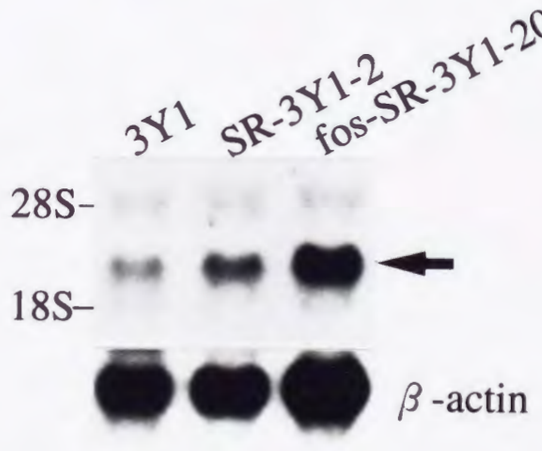
3Y1
SR-3Y1-2
fos-SR-3Y1-202
28S–
18S–
β-actin

Fig. 3 Western blot analyses. Immunoblotting of rat fibroblastic cell lines 3Y1, SR-3Y1-2 and fos-SR-3Y1-202 using anti-TM5/TM30nm antiserum (RTM8-2) and anti-actin antiserum (anti-actin). Increased levels of TM5/TM30nm protein (arrow in the right column) are found in the transformed cells (SR-3Y1-2 and fos-SR-3Y1-202) compared to that in the parental 3Y1 cells. Another extra band (arrowhead on the right column) at 32.5-kDa was also observed, particularly in the transformed cells (SR-3Y1-2 and fos-SR-3Y1-202), suggesting that this protein may be a transformation-associated protein. Reaction with anti-actin antiserum yielded a single band (arrowhead on the left column) for all of the cell lines examined, and expression levels of actin did not differ among the cell lines, suggesting that the amount of protein loaded was almost the same in each lane.

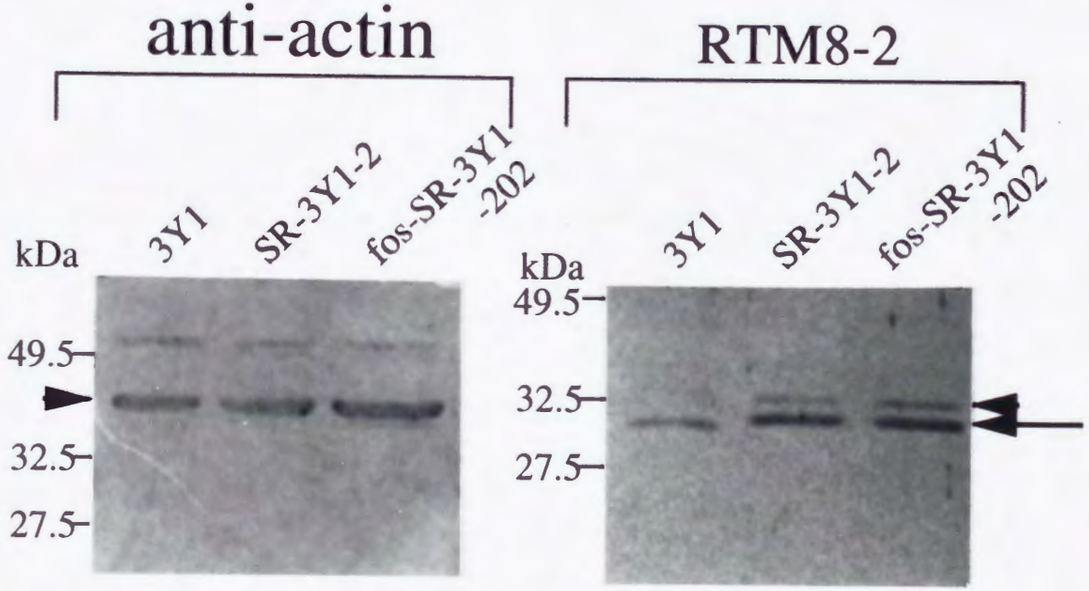
anti-actin
RTM8-2
3Y1
SR-3Y1-2
fos-SR-3Y1 -202
kDa
49.5
32.5
27.5
3Y1
SR-3Y1-2
fos-SR-3Y1 -202
kDa
49.5
32.5
27.5

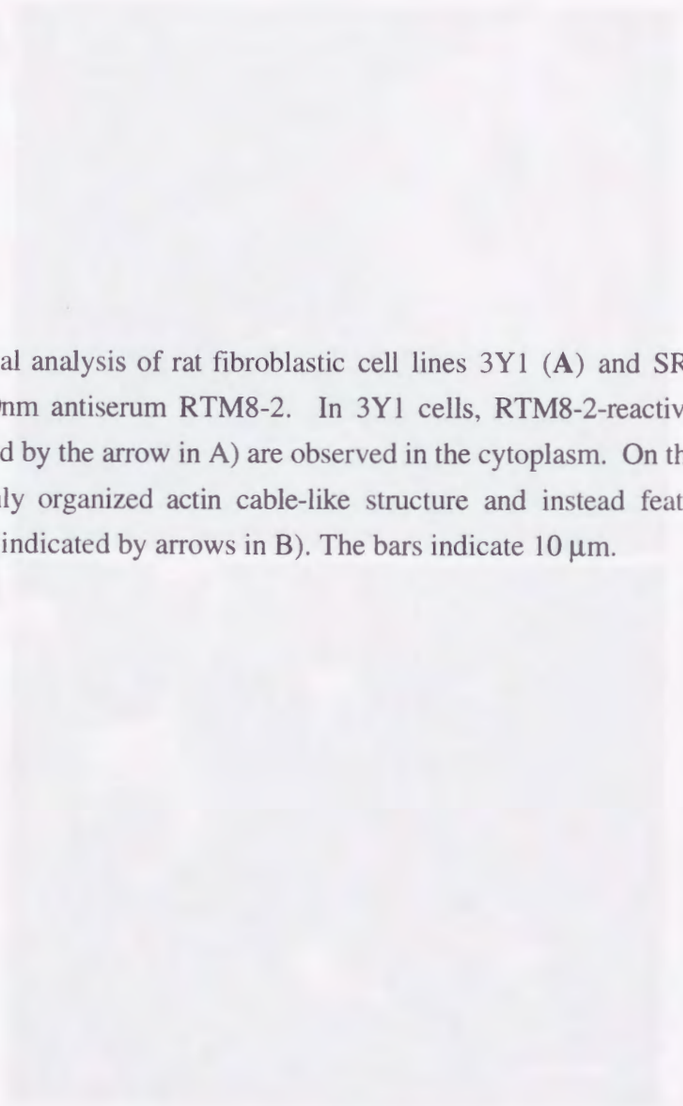

Fig. 4 Immunohistochemical analysis of rat fibroblastic cell lines 3Y1 (**A**) and SR-3Y1-2 (**B**), using the anti-rat TM5/TM30nm antiserum RTM8-2. In 3Y1 cells, RTM8-2-reactive bundles of actin microfilaments (indicated by the arrow in A) are observed in the cytoplasm. On the other hand, SR-3Y1-2 cells lost the highly organized actin cable-like structure and instead featured dot-like structures in their cytoplasm (indicated by arrows in B). The bars indicate 10 μm.

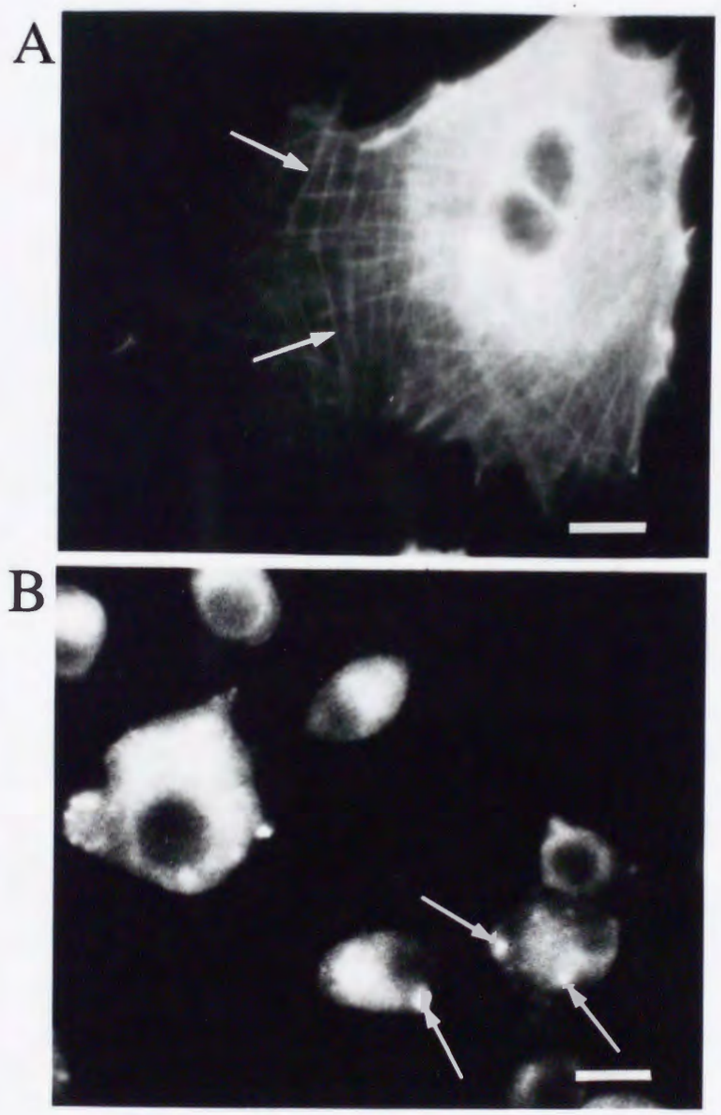
A
B

Decreased expression of a single tropomyosin isoform, TM5/TM30nm, results in reduction in motilityy of highly metastatic B16-B10 mouse melanoma cells

Abstract Tropomyosin is an actin-associated cytoskeletal protein expressed in muscle and non-muscle cells. There are several tropomyosin isoforms, and their cellular expression is known to be associated with transformation events caused by retroviral infection and chemical mutagens. We found that expression of a low-molecular weight tropomyosin isoform, TM5/TM30nm, was higher in a high-metastatic B16 mouse melanoma cell line, B16-F10, than in B16-F1, a low-metastatic mouse melanoma cell line. In order to determine whether this elevated level of TM5/TM30nm plays a role in malignant phenotype, B16-F10 cells were transfected with recombinant DNA containing antisense rat TM5/TM30nm cDNA linked to the human metallothionein-IIa promoter, which is inducible by heavy metals such as zinc and cadmium. When the stably transfected clones were treated with $ZnSO_4$, decreased expression of TM5/TM30nm and reduction in cell motility, which is thought to be an indicator of cellular malignancy, were observed. These findings suggest that TM5/TM30nm plays a fundamental role in regulating cell motility, which is essential for metastasis and invasion of tumor cells.

Introduction

Tropomyosins (TMs) are actin-associated cytoskeletal proteins of muscle and non-muscle cells and integral components of the actin-based contractile apparatus. Multiple isoforms of TMs are found in vertebrate non-muscle cells (56, 57, 58). These non-muscle TM isoforms differ in size, from the 284 residues typical of muscle TMs, the so-called high-molecular weight TMs including TM1, TM2 and TM3, to 248 residues (56), the so-called low-molecular weight TMs including TM4, TM5a, TM5b and TM30nm (also termed TM5 for mouse; hereafter referred to as TM5/TM30nm), which is ubiquitously expressed in non-muscle cells. These different isoforms are encoded by a multigene family, and in mammals four TM genes have been characterized. TM5/TM30nm is encoded by a single gene located on a chromosomal locus different from those of other TM genes, and thus is probably regulated in a different manner from the other TM genes (59).

Although it can be expected that each isoform has unique functional characteristics, e.g., for actin-binding and polymerization, this has yet to be demonstrated. In yeast, disruption of a TM gene results in reduced growth rate, heterogeneity in cell size, and disruption of actin cables (60). These findings suggest that TM plays a structural and/or regulatory role in the organization of microfilaments. In mammals, numerous studies have suggested that decrease in expression of TMs, particularly the isoforms of apparently high-molecular weight TMs, accompanies disorganization of

microfilaments and changes in morphology in cultured cells transformed by oncogenic viruses, such as SV40 and the Rous sarcoma virus (57,61-70). In addition, transfection of TMs including TM1 and TM2 into viral oncogene-transformed rodent cells suppresses tumorigenic phenotypes (71,72). These observations suggest that down-regulation of TM synthesis is related to the microfilament aberrations observed in diverse types of tumor cells (58). However, there has been no report of changes in phenotypes associated with tumorigenic transformation by transfection of low-molecular weight TMs.

In this study, we found that expression of TM5/TM30nm, a low-molecular weight TM isoform, was higher in a high-metastatic B16 mouse melanoma cell line, B16-F10, than in B16-F1, a low-metastatic mouse melanoma cell line. In order to determine whether malignant phenotype of B16-F10 cells can be reversed when the level of TM5/TM30nm is reduced, rat TM5/TM30nm cDNA was isolated and used for transfection of B16-F10 melanoma cells in an antisense orientation. We observed for transfectants carrying antisense TM5/TM30nm cDNA a decrease in expression of endogenous TM5/TM30nm protein and reduction in cell motility, which is considered an indicator of cellular malignancy (73).

Materials and Methods

Cell culture. B16-F1 and B16-F10 mouse melanoma cell lines, whose origin and properties were previously described by Fidler et al. (74), were grown at 37°C in Dulbecco's modified Eagle's medium (DMEM) supplemented with 10% fetal bovine serum (FBS) and bicarbonate (3.7 g/litter) in a moist atmosphere of 10% CO_2 and 90% air.

Construction of antisense TM5/TM30nm expression vector. For construction of the antisense TM5/TM30nm expression vector, we used rat TM5/TM30nm cDNA (termed clone #11). This cDNA was isolated from a rat macrophage cDNA library (Clontech, CA) using a probe for a 0.8-kilobase pairs (kb) 3' untranslated region (3'-UTR) of mouse TM5 cDNA, which was kindly provided by Dr. Shigeru Sakiyama (Chiba Cancer Center, Chiba, Japan). The isolated rat TM5/TM30nm cDNA was 1,770 bp in size and contained 65 and 970 bp nucleotides (nt) of 5' and 3' untranslated sequence, respectively (manuscript in preparation; accession number X72859). During the cloning, we were familiar with a report of the isolation and characterization of rat TM5/TM30nm gene (termed *rTMnmNM-1*) (75). The rat TM5/TM30nm exhibited 99.6% amino acid homology with the *rTMnmNM-1* coding sequence, in which only the 83th amino acid was different, i.e., Val (GTT) in rat TM5/TM30nm and Ala (GCT) in *rTMnmNM-1*. The predicted open

reading frame encoded 248 amino acids, 2 amino acids (fourth and 83th) of which differed among species, i.e., the fourth amino acid was Ser (AGC) in rats, Thr (ACC) in mice and Ile (ATC) in humans, and the 83th amino acid was Val (GTT) in the rat we used, Ala (GCT) in mice (76) and humans (65). Harrplot analysis revealed high degrees of similarity (76.0 and 92.9%, respectively) to human and mouse counterparts at the nucleic acid level, as expected. This finding encouraged us to use the rat TM5/TM30nm cDNA as a source for suppression of mouse TM5/TM30nm mRNA synthesis by antisense technology, since antisense rat GLUT-2 cDNA, which has 94% homology with mouse GLUT-2 cDNA, has been reported to suppress endogenous mouse GLUT-2 mRNA synthesis *in vivo* (77). The 807-base pairs (bp) fragment digested with *Eco*RI and *Acc*I of clone #11 was blunt-ended and inserted into the *Hin*dIII site (which had previously been destroyed) of pMEP4 plasmid vector (78), which possesses the EBNA (EB virus-associated nuclear antigen I) sequence (which allows pMEP4 to replicate as an episome in eukaryotic cells), hygromycin-resistant gene ($Hygr^R$) (conferring resistance to hygromycin B) and human metallothionein-IIa promoter. The resulting vector with the insert in reverse orientation was designated antisenseTM, and that with the insert in sense orientation was designated senseTM (Fig. 1). SenseTM vector and mock (pMEP4 alone) were used as negative controls.

Transfection and selection of transfectants. For transfection, CsCl-purified vector DNA (10 μg in a circular form) was co-precipitated with Ca-phosphate using the method of Sadano et al. (79). The precipitated DNA was transfected into $5X10^5$ cells in a 60mm tissue culture dish (Corning Coster, MA). After transfection, cells were washed with DMEM and cultured in the presence of 400 μg/ml of hygromycin B (Sigma Chem. Co., MI) for 6 days. Independent clones surviving culture in hygromycin B were picked up from each of 3 dishes and propagated for PCR analysis, and then frozen in liquid nitrogen prior to use for Western blot analysis and for cell motility assay. Frozen-thawed clones were cultured in the absence (control) or presence of 600 μM $ZnSO_4$ (Nakarai Tesque, Kyoto, Japan) for 2 h and then subjected to the analyses mentioned above.

PCR analysis. One set of oligonucleotide primers, hyg-S and hyg-RV, was synthesized using a 380A DNA synthesizer (Perkin Elmer, Foster City, CA). Hyg-S is 5'-TCA GCT TCG ATG TAG GAG GG-3' (corresponding to positions 320 to 339 of the $Hygr^R$ sequence (80), and hyg-RV is 5'-AAC ATC GCC TCG CTC CAG TC-3' (positions 875 to 856). The size of the product was designed to amplify a 556-bp region of $Hygr^R$. Amplification was performed in a 25 μl reaction mixture containing 0.5-1.0 μg of genomic DNA, 2.5 μl of 10X PCR buffer, 1 μl of each primer (5 μM), 2 μl of 10 mM dNTPs, 0.125 μl of *Taq* polymerase (Takara Shuzo Co., Ltd., Tokyo, Japan) and dH_2O with a DNA Thermal Cycler (Biometra, Göttingen, Germany). The mixture was heated to 94°C for 45 sec (denaturation), cooled to 50°C for 25 sec (annealing) and heated at 72°C for 3 min (extension) for 30 amplification cycles. Five μl of the PCR product was subjected to electrophoresis

on a 2% agarose gel. Amplified sequences were identified by ethidium bromide staining under ultraviolet illumination, and photographed.

Northern blot hybridization. Total RNA was isolated by the guanidium thiocyanate method (81). RNA (20 μg/lane) was electrophoresed on a 1.5% agarose/formaldehyde gel and blotted onto a nitrocellulose filter membrane (S&S GmbH, Dassel, Germany). RNA blotting was performed as previously described (81). The filter membrane was then hybridized with an $\alpha[^{32}P]$-dCTP-labeled 0.8-kb 3'-UTR of mouse TM5/TM30nm cDNA. Signals for positive hybridization were quantified using a densitometer (DH303, Advantec, CA).

Immunoblotting analysis. Anti-TM5/TM30nm antiserum, termed RTM8-2 (82), was prepared by immunizing rabbits with an oligopeptide (^{233}CTQRMLDQTLLDLNEM^{248}) corresponding to the C-terminal region of rat TM5/TM30nm; this region is completely conserved among human, rat and mouse (10,21). Proteins (20 μg per lane) were electrophoresed and immunoblotted onto nitrocellulose filters (S&S GmbH) that had been immersed in RTM8-2 (diluted 1: 500), as previously described (83). Positive signals were quantified using the densitometer.

Quantitative measurement of cell motility. Cells were seeded onto 60mm tissue culture dishes (Corning) ($4X10^5$ cells per dish) and cultured for 36-38h. In some cases, $ZnSO_4$ was added to the culture media to a final concentration of 600 μM, and incubated for an additional 2 h. Cell motility was then measured using a method based on trace images obtained by video-image analyses and computer techniques (73). Briefly, microscopical images of cells were obtained by accumulating eight frames at 20 sec intervals using Allen video-enhanced contrast-differential interference contrast (AVEC-DIC) microscopy (84). The quantitative value of motility was defined as a motility index (MI).

$$MI=(\sum_{n=1}^{m} In-\sum_{n=1}^{m} In^*)/N\,m$$

where In is the intensity of a trace image for any one video frame, $\sum_{n=1}^{m} In$ is the result of accumulation and $\sum_{n=1}^{m} In^*$ is for image without cells (mainly including electric noise). Then, $(\sum_{n=1}^{m} In-\sum_{n=1}^{m} In^*)/N$ can be assumed to be a function of the video frame, where N is the number of cells in a window. Here "m" is the number of accumulation of the trace images. We usually fix "m" at eight and the time interval between video frames at 20 sec. MI value is defined as cell motility per cell per video frame interval. MI values are indicated as means±SD, and obtained by recording images of cells at three to nine randomly selected spots in a dish.

Results

Difference in motility between B16-F1 and B16-F10 cells.

Since high-metastatic tumor cells have been shown to be more motile than low-metastatic cells (74), we first compared the motility of high-metastatic mouse melanoma cell line B16-F10 with that of low-metastatic mouse melanoma cell line B16-F1 using AVEC-DIC microscopy. MI values were estimated for cells cultured for 38 h in the absence of $ZnSO_4$. B16-F1 cells had lower MI values than did B16-F10 cells (Fig. 2), indicating that B16-F1 has lower cell motility than does B16-F10. This finding is consistent with previous findings that the MI values of cells exhibiting stably transformed phenotypes were higher than those of cells that had reverted to nontransformed morphology (73).

Northern blot analysis revealed a higher level (ca. 1.6-fold) of mRNA (1,800 nt in size) for TM5/TM30nm in B16-F10 cells than in B16-F1 cells (Fig. 3**A**). This was further confirmed by Western blot analysis using RTM8-2 (Fig. 3**B**). The TM5/TM30nm protein reacting with the antibody was 31 kDa in size. This size is consistent with the previous finding that human TM30nm mRNA encoded an approximately 30-kDa molecular weight polypeptide when translation products of TM30nm mRNA obtained using a cell-free system were analyzed by two-dimensional gel electrophoresis (65). The level of TM5/TM30nm protein in B16-F10 was ca. 1.8-fold higher than that in B16-F1. These findings suggest that cell motility is strongly correlated with levels of TM5/TM30nm mRNA and protein. An additional band reactive with RTM8-2 at a molecular weight above ca. 31 kDa was also detected. Identification of this peptide fragment has not been completed, although it appears to be TM2 protein, based on results of a preliminary test using two-dimensional electrophoresis (data not shown).

Reduced motility of B16-F10 cells transfected with antisense TM5/TM30nm cDNA expression vector.

B16-F10 cells, which express TM5/TM30nm at a relatively high level, were transfected with antisenseTM, senseTM and mock DNAs to test whether reduced expression of TM5/TM30nm can affect cell motility. After transfection, hygromycin-resistant clones were independently isolated from each of dishes. The presence of plasmid DNA introduced into these clones was confirmed by PCR analysis (Fig. 4**A**). When each of independent clones [including clones carrying antisenseTM

DNA (termed F10A-1 and F10A-2), clones carrying senseTM DNA (termed F10S-1, F10S-2 and F10S-3) and clones carrying mock DNA (termed F10M1 and F10M2)] was treated with $ZnSO_4$ or without $ZnSO_4$ for 2 h and then tested for cell motility, F10A-1 and F10A-2 carrying antisenseTM that had been induced with $ZnSO_4$ exhibited large reductions in motility (82 and 80%, respectively) compared with that of F10A-1 and F10A-2 cells cultured in the absence of $ZnSO_4$ (Fig. 4**B**). None of the clones carrying senseTM or mock DNA exhibited change in motility even after treatment with heavy metals (Fig. 4**B**). In Fig. 4**C**, typical video-images used to determine MI values are shown. The density of the clone (F10A-1) carrying antisenseTM was dramatically reduced after treatment with heavy metals, whereas the motility of clones carrying either senseTM or mock DNA remained unchanged.

Reduced synthesis of TM5/TM30nm in B16-F10 cells transfected with antisense TM5/TM30nm cDNA expression vector.

We next examined whether the protein level of TM5/TM30nm was reduced in $ZnSO_4$-treated F10A-1 and F10A-2 clones, both of which had also exhibited reduced motility. Cells were cultured in the presence or absence of 600 μM $ZnSO_4$ for 2 h, harvested, lysed and subjected to Western blot analysis using RTM8-2. Both clones exhibited decreased TM5/TM30nm expression (ca. 31 kDa in size) after induction with heavy metals (Fig. 5**A**). The CBB staining pattern for SDS-PAGE revealed that an equal quantity of protein had been applied to each lane (Fig. 5**B**). Densitometric scanning demonstrated 60% and 40% reductions, respectively, in TM5/TM30nm in the $ZnSO_4$-treated F10A-1 and F10A-2 cells.

Discussion

The regulation of actin-based cytoskeletal organization is complex, and numerous actin-binding proteins are involved in this process (85). Synthesis of several members of the TM family, particularly the isoforms of apparently high-molecular weight, is frequently decreased in association with neoplastic transformation by various chemical and viral agents (57,61-70), as well as in human

carcinoma cells (86,87). There have been a few reports that changes in synthesis of TMs are involved in the progression of malignancy of tumor cells, particularly as TMs involve the expression of metastatic phenotypes. For example, Takenaga et al. (86) found that synthesis of TM2 is much lower in the high-metastatic Lewis lung carcinoma cell line than in the low-metastatic counterpart. Similar findings were observed in a comparison of high-metastatic v-Ha-*ras*-transformed NIH3T3 (pH1-3) cells and low-metastatic counterpart and parental NIH3T3 cells (69). In addition, the tumorigenicity of cell lines such as NIH3T3 and v-*raf*-transformed NRK is suppressed upon constitutive expression of single cDNAs encoding cytoskeletal proteins including TM1 and TM2 (71,72). In this study, we found that an elevated level of TM5/TM30nm, one of the low-molecular weight TM family proteins, is strongly correlated with increase in motility of high-metastatic mouse melanoma cells. Similar observations were obtained for another metastatic v-*src*-transformed rat fibroblastic cell line, SR-3Y1-2 (data not shown). Matsumura et al. (62) have shown the levels of one or both of TM1 and TM2 are decreased and the levels of one or both of TM3 and TM5 are increased upon transformation by either DNA or RNA viruses. The present transfection experiment with antisense TM5/TM30nm cDNA, together with TM1 and TM2, shows that reversion of TM isoform to the normal level is able to partially suppress the transformed phenotype.

Transformed cells differ from normal cells more by the conspicuous absence of higher ordered structures of microfilaments than by an absence of microfilaments themselves (62). It seems possible that changes in the composition of microfilaments could be responsible for the change in the organization of stress fibers upon cell transformation. Therefore, the cellular phenotype is closely related to the integrity of microfilaments and thus depends on the expression of the actin-related molecules (88,89). Matsumura et al. (62) have found changes in the patterns of tropomyosin in the microfilaments in many cell types during cellular transformation and suggested that TM5 is involved in destabilization of microfilaments, while high-molecular weight TMs promote organization of microfilaments.

It should be noted that the amount of extra band above 31 kDa TM5/TM30nm protein, presumbaly TM2, significantly increased by the treatment with $ZnSO_4$ (see Fig. 5A). Schevzov et al. (90) pointed out that the pattern of TM gene expression may change in response to

cytoarchitectural changes *via* a feedback mechanism. Thus, the reduced expression of TM5/TM30nm caused by antisense gene expression may affect the amount of other TMs such as TM2, which in turn accelerates reduction in motility of B16-F10 cells.

It is also interesting to note that F10A-1 and F10A-2 showed the same extent of cell motility, although F10A-1 expressed more TM5/TM30nm than did F10A-2 (see Fig. 4B, 5A). This suggests the presence of threshold with respect to the amount of TM5/TM30nm which may cause microfilament disorganization. In our case, a slight difference in the amount of TM5/TM30nm was observed in F10A-1 and F10A-2 cells, but the levels of TM5/TM30nm in both cells appeared to be enough low not to disorganize cellular microfilament organization which reflects cell motility.

A few attempts to suppress the production of endogenous cytoskeletal proteins have been made. Elimination of one protein, vinculin or TM1, by antisense RNA expression induces the characteristics of malignant tumors in two cell lines, 3T3 cells and chemically immortalized Syrian hamster embryonic cells, respectively (91,92). These observations, together with ours, will be useful for development of antisense-mediated gene therapy to suppress the progression of malignant tumors.

References

56. Cote, G.P. (1983) Structural and functional properties of the non-muscle tropomyosins. Mol. Cell. Biochem. **57**, 127-146.
57. Lin, J. J.-C., Helfman, D.M., Hughes, S.H. and Chou, C.-S. (1985) Tropomyosin isoforms in chicken embryo fibroblasts: purification, characterization and changes in Rous sarcoma virus-transformed cells. J. Cell. Biol. **100**, 692-703.
58. Matsumura, F. and Yamashiro-Matsumura, S. (1986) Modulation of actin-bundling activity of 55-kDa protein by multiple isoformes of tropomyosin. J. Biol. Chem. **261**, 4655-4659.
59. Clayton, L., Reinach, F.C., Chumbley, G.M. and MacLeod, A.R. (1988) Organization of the hTMnm gene: Implications for evolution of muscle and non-muscle tropomyosins. J. Mol. Biol. **201**, 507-515.
60. Liu, H. and Bretscher, A. (1989) Disruption of the single tropomyosin gene in yeast results in the disappearance of actin cables from the cytoskeleton. Cell **57**, 233-242.

61. Leonardi, C.L., Warren, R.H. and Rubin, R.W. (1982) Lack of tropomyosin correlates with the absence of stress fibers in transformed rat kidney cells. Biochem. Biophys. Acta **720**, 154-162.

62. Matsumura, F., Lin, J. J.-C., Yamashiro-Matsumura, S., Thomas, G.P. and Topp, W.C. (1983) Differential expression of tropomyosin isoforms in the microfilaments isolated from normal and transformed rat cultured cells. J. Biol. Chem. **258**, 13954-13964.

63. Hendricks, M. and Weintraub, H. (1984) Multiple tropomyosin polypeptides in chicken embryo fibroblasts: differential repression of transcription by Rous sarcoma virus transformation. Mol. Cell. Biol. **4**, 1823-1833.

64. Cooper, H.L., Feuerstein, N., Noda, M. and Bassin, R.H. (1985) Suppression of tropomyosin synthesis, a common biochemical feature of oncogenesis by structurally diverse retroviral oncogenes. Mol. Cell. Biol. **5**, 972-983.

65. MacLeod, A.R., Houlker, C., Reinach, F.C. and Talbot, K. (1986) The mRNA and RNA-copy pseudogenes encoding TM30nm, a human cytoskeletal tropomyosin. Nucleic Acid Res. **14**, 8413-8426.

66. Cooper, H.L., Bhattacharya, B., Bassin, R.H. and Salomon, D.S. (1987) Suppression of synthesis and utilization of tropomyosin in mouse and rat fibrobrasts by transforming growth factor-alpha: a pathway in oncogene actin. Cancer Res. **47**, 4493-4500.

67. Leavitt, J., Latter, G., Lutomski, L., Goldstein, D. and Burbeck, S. (1986) Tropomyosin isoform switching in tumorigenic human fibroblasts. Mol. Cell. Biol. **6**, 2721-2726.

68. Lin, C.-S. and Leavitt, J. (1988) Cloning and characterization of a cDNA encoding transformation-sensitive tropomyosin isoform 3 from tumorigenic human fibroblassts. Mol. Cell. Biol. **8**, 160-168.

69. Takenaga, K., Nakamura, Y. and Sakiyama, S. (1988) Suppression of synthesis of tropomyosin isoform 2 in metastatic v-Ha-ras-transformed NIH3T3 cells. Biochem. Biophys. Res. Commun. **157**, 1111-1116.

70. Varma, M. and Leavitt, J. (1988) Macromolecular changes accompanying immortalization and tumorigenic conversion in a human fibroblast model system. Mutat. Res. **199**, 437-447.

71. Prasad, G.L., Fuldner, R.A. and Cooper, H.L. (1993) Expression of transduced tropomyosin 1 cDNA suppresses neoplastic growth of cells transformed by the ras oncogene. Proc. Natl. Acad. Sci. USA **90**, 7039-7043.

72. Takenaga, K. and Masuda, A. (1994) Restoration of microfilament bundle organization in v-raf-transformed NRK cells after transduction with tropomyosin 2 cDNA. Cancer Lett. **87**, 47-53.

73. Tatsuka, M., Jinno, S. and Kakunaga, T. (1989) Quantitative measurement of cell motility associated with transformed phenotype. Jpn. J. Cancer Res. **80**, 408-412.

74. Fidler, I.J., Gersten, D.M. and Hart, I.R. (1978) The biology of cancer invasion and metastasis. Adv. Cancer Res. **28**, 149-250.

75. Beisel, K.W. and Kennedy, J.E. (1994) Identification of novel alternatively spliced isoforms of the tropomyosin-encoding gene, *TMnm*, in the rat cochlea. Gene **143**, 251-256.

76. Takenaga, K., Nakamura, Y., Kageyama, H. and Sakiyama, S. (1990) Nucleotide sequence of cDNA for nonmuscle tropomyosin 5 of mouse fibroblast. Biochem. Biophys. Acta **1087**, 101-103.

77. Valera, A., Solanes, G., Fernández-Alvarez, J., Pujol, A., Ferrer, J., Asins, G., Gomis, R. and Bosch, F. (1994) Expression of GLUT-2 antisense RNA in beta cells of transgenic mice leads to diabetes. J. Biol. Chem. **269**, 28543-28546.

78. Gupta, S.L., Charlin, J.M., Pyati, P., Dai, W., Pfefferkorn E.R. and Murphy, M.J.Jr. (1994) Antiparasitic and antiproliferative effects of indoleamine 2,3-dioxygenase enzyme expression in human fibroblasts. Infect. Immun. **62**, 2277-2284.

79. Sadano, H., Taniguchi, S. and Baba, T. (1990) Newly identified type of β actin reduces invasiveness of mouse B16-melanoma. FEBS Lett. **271**, 23-27.

80. Gritz, L. and Davies, J. (1983) Plasmid-encoded hygromycin B resistance: the sequence of hygromycin B phosphotransferase gene and its expression in Escherichia coli and Saccharomyces cerevisiae. Gene **25**, 179-188.

81. Sambrook, J., Fritsch, E.F. and Maniatis T. (1989) "Molecular cloning: a laboratory mannual," 2nd edn., Cold Spring Harbor Laboratory, Cold Spring Harbor, NY.

82. Miyado, K., Katsuki, M. and Taniguchi, S. (1994) Isolation of a yeast tropomyosin-related cDNA clone that encodes a novel transmembrane protein having a C-terminal highly basic region. Biochem. Biophys. Res. Commun. **199**, 1363-1371.

83. Okamoto-Inoue, M., Taniguchi, S., Sadano, H., Kawano, T., Kimura, G., Gabbiani, G. and Baba, T. (1990) Alteration in expression of smooth muscle α-actin associated with transformation of rat 3Y1 cells. J. Cell Sci. **96**, 631-637.

84. Allen, R.D., Allen, N.S. and Travis, J.L. (1981) Video-enhanced contrast, differential interference contrast (AVEC-DIC) microscopy: a new method capable of analyzing microtuble-related motility in the reticulopodial network of allogromia laticollaris. Cell Motil. **1**, 291-302.

85. Luna, E.J. and Hitt, A.L. (1992) Cytoskeleton-plasma membrane interactions. Science **25**, 955-964.

86. Takenaga, K., Nakamura, Y. and Sakiyama, S. (1988) Isolation and characterization of a cDNA that encodes mouse fibroblast tropomyosin isoform 2. Mol. Cell. Biol. **8**, 3934-3937.

87. Bhattacharya, B., Prasad, G.L., Valverius, E.M., Salomon, D.S. and Cooper, H.L. (1990) Tropomyosins of human mammary epithelial cells: consistent defects of expression in mammary carcinoma cell lines. Cancer Res. **50**, 2105-2112.

88. Sadano, H., Inoue, M. and Taniguchi, S. (1990) Differential expression of vinculin between weakly and highly metastatic B16-melanoma cell lines. Jap. J. Cancer Res. **83**, 625-630.

89. Shimokawa-Kuroki, R., Sadano, H. and Taniguchi, S. (1994) A variant actin (βm) reduces metastasis of mouse B16 melanoma. Int. J. Cancer **56**, 689-697.

90. Schevzov, G., Lloyd, C., Hailstones, D. and Gunning, P. (1993) Differential regilation of tropomyosin isoform organization and gene expression in response to altered actin gene expression. J. Cell Biol. **121**, 811-821.

91. Rodríguez Fernández, J.L., Geiger, B., Salomon, D.S., Sabanay, I., Zoller, M. and Ben-Zé ev, A. (1992) Suppression of tumorigenicity in transformed cells after transfection with vinculin cDNA. J. Cell Biol. **122**, 1285-1294.

92. Boyd, J., Risinger, J.I., Wiseman, R.W., Merrick, W.B., Selkirk, J.K. and Barrett, J.C. (1995) Regulation of microfilament organization and anchorage-independent growth by tropomyosin 1. Proc. Natl. Acad. Sci. USA **92**, 11534-11538.

Footnotes

Abbreviations: TMs, tropomyosins; UTR, untranslated region; EBNA, EB virus-associated nuclear antigen I; $Hygr^R$, hygromycin-resistant gene; MI, motility index

Figure legends

Fig. 5 Schematic representation of expression vectors for sense and antisense TM5/TM30nm RNA. A 807-bp *Eco*RI-*Acc*I fragment containing rat TM5/TM30nm cDNA was inserted into the *Hin*dIII site of pMEP4 in a sense or antisense orientation. The resulting vectors carrying sense or antisense TM5/TM30nm cDNA were designated senseTM and antisenseTM, respectively. pMEP4 without an insert was used as a mock DNA. The shaded boxes in the inserts indicate the coding region of TM5/TM30nm cDNA. Parentheses indicate the restriction enzyme sites destroyed. The number given at some restriction enzyme sites indicates the number of nucleotide position for pMEP4 (23). Amp^R, β-lactamase gene; EBNA-1, EB virus-derived nuclear antigen-1; $Hygr^R$, hygromycin-resistant gene; OriP, replication origin; PhMTIIa, promoter of human metallothionein-IIa gene; PTK, promoter of herpes simplex virus thymidine kinase gene; SVpA, poly (A) signal of SV40 virus early gene; TKpA, poly (A) signal of herpes simplex virus thymidine kinase gene.

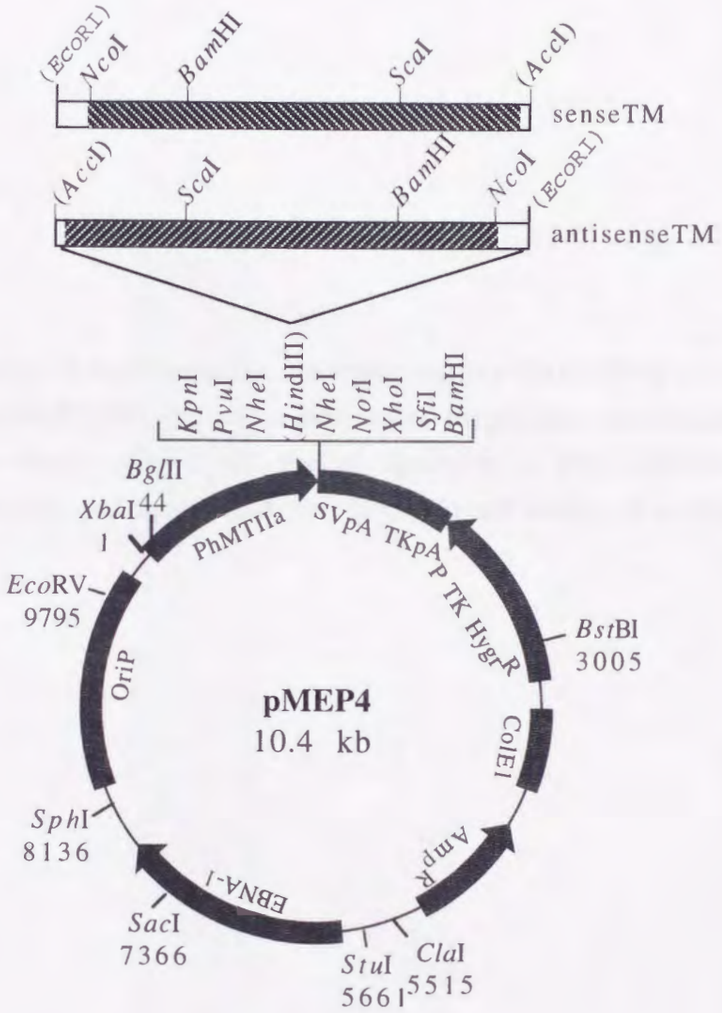
(EcoRI)
NcoI
BamHI
ScaI
(AccI)
senseTM
(AccI)
ScaI
BamHI
NcoI
(EcoRI)
antisenseTM
KpnI
PvuI
NheI
(HindIII)
NheI
NotI
XhoI
SfiI
BamHI
BglII
XbaI 44
1
PhMTIIa
SVpA
TKpA
P TK HygR
BstBI
3005
EcoRV
9795
OriP
pMEP4
10.4 kb
CoIE1
AmpR
SphI
8136
EBNA-1
SacI
7366
StuI
5661
ClaI
5515

Fig. 6 Comparison of motility of high-metastatic melanoma cell line B16-F10 (F10) and low-metastatic melanoma cell line B16-F1 (F1). MI values indicated on the abscissa were measured for a total of three independent portions for each cell line as described in **MATERIALS AND METHODS**. B16-F10 cells displayed significant higher ($P<0.05$) cell motility than did B16-F1 cells.

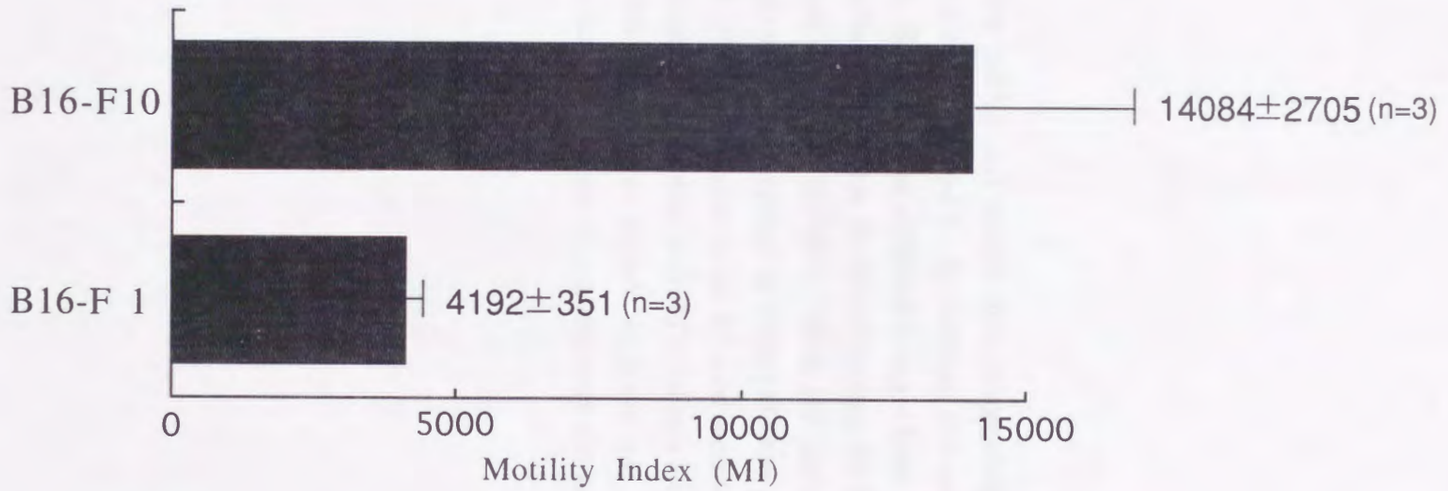
B16-F10
14084±2705 (n=3)
B16-F 1
4192±351 (n=3)
0
5000
10000
15000
Motility Index (MI)

Fig. 7 Expression of TM5/TM30nm mRNA and protein in high-metastatic melanoma cell line B16-F10 and low-metastatic melanoma cell line B16-F1. **A**, Northern blot analysis using a 0.8-kb mouse TM5/TM30nm 3'-UTR probe. Both cell lines exhibited a single band with 1,800 nt in size (arrowhead), although intensity of the band was higher for B16-F10 than for B16-F1. **B**, Western blot analysis using anti-TM5/TM30nm antiserum, RTM8-2. Both cell lines exhibited a positive band at ca. 31 kDa in size (arrowhead) which corresponds to TM5/TM30nm protein. The intensity of the band in the sample of B16-F10 cells was found to be ca. 1.8-fold increased compared with in the sample of B16-F1 cells. An additional band reactive with RTM8-2 at a molecular weight above ca. 31 kDa was also detected. Identification of this peptide fragment has not been completed, although it appears to be TM2 protein, based on results of a preliminary test using two-dimensional electrophoresis (data not shown).

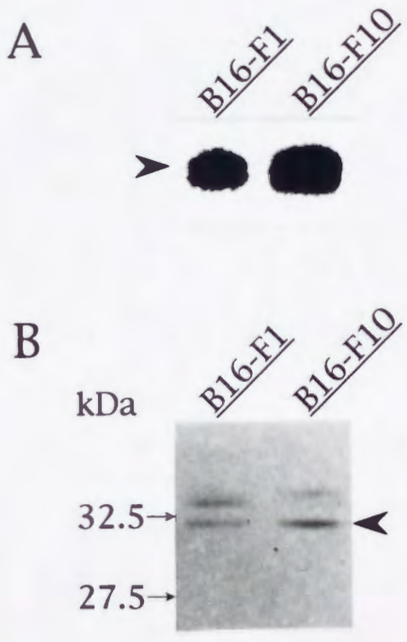
A
B16-F1
B16-F10
B
kDa
B16-F1
B16-F10
32.5
27.5

Fig. 8 PCR analysis and cell motility test of B16-F10 transfectants. **A**, PCR analysis of genomic DNA from B16-F10 transfectants carrying antisenseTM DNA (F10A-1 and F10A-2), B16-F10 transfectants carrying senseTM DNA (F10S-1, F10S-2 and F10S-3) and B16-F10 transfectants carrying mock DNA (F10M1 and F10M2). B16-F10 indicates the sample of cell line, which had no exogenous DNA. Template (-) indicates a sample that PCR-reaction was done without genomic DNA. The expected band at 556 bp (indicated by arrowhead) was found for all transfectants. **B**, MI values for B16-F10 transfectants after culture in the presence [Zn (+)] or absence [Zn (-)] of 600 μM $ZnSO_4$ for 2 h. MI values indicated on the abscissa were measured for a total of 9 portions for each cell line. **C**, Trace images of typical transfectants carrying antisenseTM DNA, senseTM DNA and mock DNA after culture in the presence (Zn+) or absence (Zn-) of 600 μM $ZnSO_4$ for 2 h. Cells transfected with antisenseTM DNA exhibited a dramatic decrease in motility after induction with heavy metals.

A

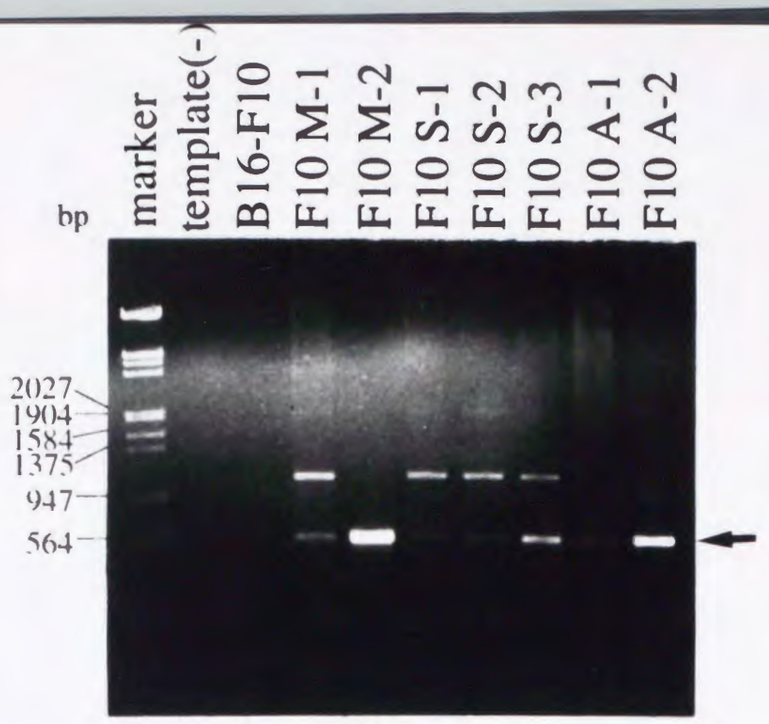
bp
marker
template(-)
B16-F10
F10 M-1
F10 M-2
F10 S-1
F10 S-2
F10 S-3
F10 A-1
F10 A-2
2027
1904
1584
1375
947
564

B

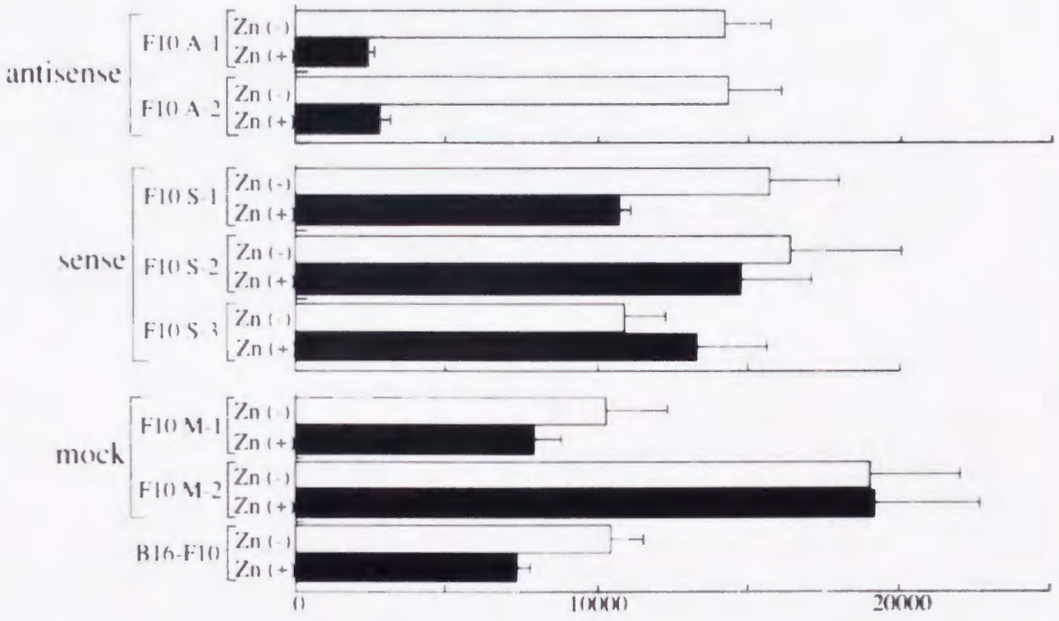
antisense
F10 A-1
F10 A-2
sense
F10 S-1
F10 S-2
F10 S-3
mock
F10 M-1
F10 M-2
B16-F10
Zn (-)
Zn (+)
0
10000
20000

C

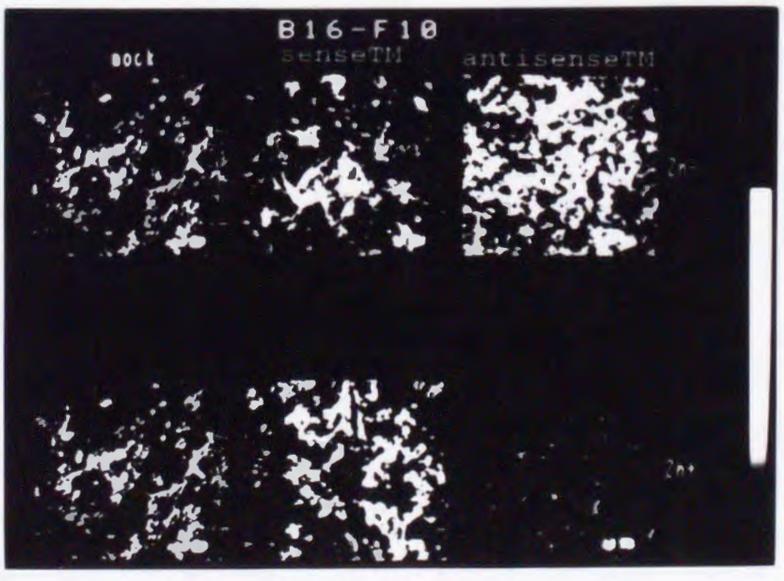
B16-F10
mock
senseTM
antisenseTM
Zn-
Zn+

Fig. 9 Expression of TM5/TM30nm protein in B16-F10 transfectants (F10A-1 and F10A-2) carrying antisenseTM DNA after culture in the presence (+) or absence (-) of 600 μM $ZnSO_4$ (Zn^{2+}) for 2 h. **A**, Western blot analysis using anti-TM5/TM30nm antiserum, RTM8-2. Both cell lines exhibited decreased levels of 31-kDa TM5/TM30nm protein (indicated by arrowhead) in the presence of $ZnSO_4$. **B**, CBB staining pattern for SDS-PAGE prior to immunoblotting by RTM8-2. Stain shows that comparable amount of protein was applied to each lane.

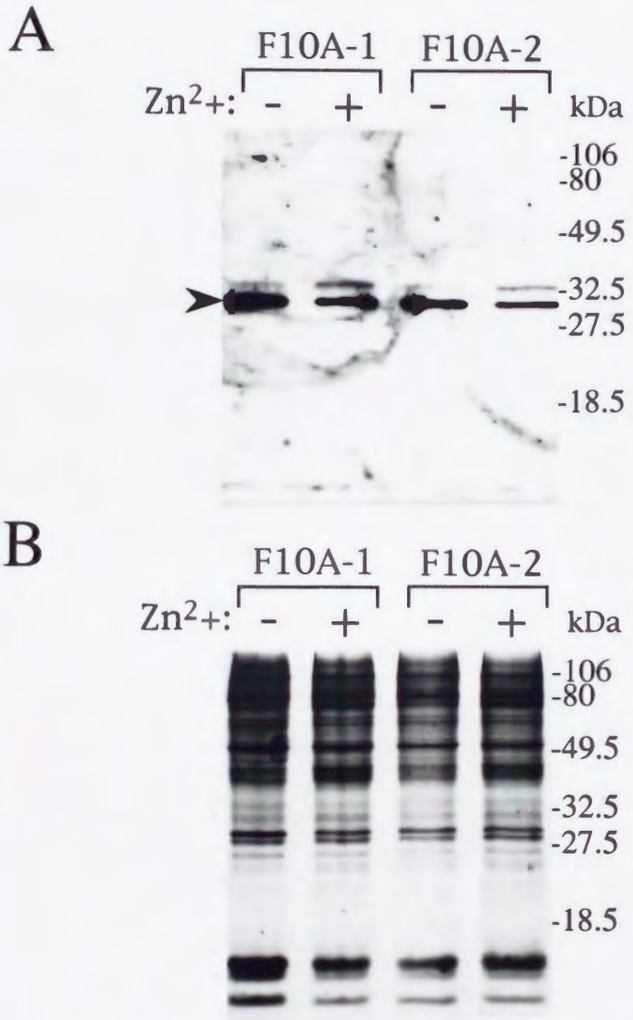
A
F10A-1
F10A-2
Zn2+: - + - +
kDa
-106
-80
-49.5
-32.5
-27.5
-18.5
B
F10A-1
F10A-2
Zn2+: - + - +
kDa
-106
-80
-49.5
-32.5
-27.5
-18.5

Isolation of a yeast cDNA clone that encodes a novel transmembrane protein having C-terminal highly basic region

Abstract A novel cDNA clone was isolated from a yeast Saccharomyces cerevisiae λgt11 cDNA library using rabbit anti-rat TM30nm polyclonal antibody (RTM8-2). It consists of an open reading frame of 951 bp, encoding 317 amino acid residues. The putative sequence recognized by RTM8-2 was present in Asn-235 to Thr-250. The deduced amino acid sequence and hydropathy plot suggested that this protein has a tropomyosin-homologous sequence, a predicted transmenbrane, and a C-terminal basic region. A search of the data bases (EMBL and GenBank) revealed that the 128bp sequence in the 3' untranslated region (3'UTR) is almost identical (96.9%) to the human cDNA clone 54E05 sequence (EMBL accession number Z15978).

Introduction

We isolated a rat tropomyosin TM30nm partial cDNA clone, and established the anti-TM30nm antibody (RTM8-2). TM30nm is one of non-muscle tropomyosins. Clayton et al. (93) have previously isolated hTMnm gene encoding TM30nm, and clarified that this gene family consists of a single structural gene which is independent of other tropomyosin families. The expression of a protein recognized by RTM8-2 was observed in several cell lines and tissues, as well as in yeast S.cerevisiae. Therefore, to examine the function of TM30nm in yeast, cDNA cloning was performed to identify any yeast TM30nm related proteins.

Materials and Methods

Antiserum Preparation and Western Blotting. We isolated a rat TM30nm partial cDNA clone (Fig.1A), and synthesized the rat TM30nm C-terminal oligopeptide (233CTQRMLDQTLLDLNEM248), and conjugated it with key holl limpet hemocyanin (KLH). The oligopeptide was subcutaneously injected three times into a rabbit (KBL: JW, 10-week-old male), and then the antiserm was collected 73 days later. The obtained antibody was designated as RTM8-2. All the protein samples were prepared from rat (WKA, ♀) normal spleen and heart tissues, and S.cerevisiae (SEY 6210 strain), and the immunoblotting was performed as described (94). The nitrocellurose filters were immersed in anti-actin monoclonal antibody (N350) (1:500) (Amersham, UK), anti-tropomyosin polyclonal antibody (T3651) (1:500) (Sigma Chemical Co., StLouis, MO), or RTM8-2 (1:500).

cDNA Cloning and Sequencing. RTM8-2 was used to screen a λ gt11 S.cerevisiae cDNA library (Clontech). The screening method was based on the technique described by Sambrook et al.(95). The cDNA inserts were subcloned to the EcoRI site of pBlucescript SK(+). The cDNA sequence was determined by the dideoxy chain termination method (96). The search and analysis of

the EMBL, GenBank, and SwissProt data bases as well as the motif was performed using the Gene Works 2.2.1 software package (IntelliGenetics, Inc., USA).

Zoo Blotting. For Zoo blotting, genomic DNAs were extracted from several sources in different organisms (yeast, rat, and human) as described (97). The blots were prepared using BamHI-digested DNA from yeast S.cerevisiae (Clontech), a rat (brain and liver), a human (Hela cells and Placenta (Clontech)), and fragmentation products were separated by electrophoresis in 0.6% agarose gels in 0.5× TBE buffer, followed by a capillary transfer to nylon menbranes (Hybond N) in 10× SSC (1× SSC is 0.15M NaCl, 0.015M sodium citrate). Hybridization was performed using the [32P]CTP-labelled pY34 DraI-XbaI fragment as the probe.

Results and Discussion

The immunoblotting of the yeast S.cerevisiae extract was performed with several cytoskeletal protein antibodies: monoclonal mouse anti-actin antibody (N350) (Amersham, UK), polyclonal rabbit anti-tropomyosin antibody (T3651) (Sigma Chemical Co., St Louis, MO), and anti-TM30nm antibody (RTM8-2). Both rat spleen and heart tissue specimens were used as the positive and negative control samples, respectively (Fig.1A). When compared with the previous report of other groups (98,99), S.cerevisiae actin and tropomyosin were detected by each antibody. On the other hand, the protein recognized by RTM8-2 was more slowly mobilized than the hitherto known yeast tropomyosins (99,100). To identify this protein, cDNA cloning was performed using RTM8-2 as the first antibody.

As shown in Fig.2A, several overlapping cDNA clones (pY5, pY6, pY29, and pY34) were isolated from the S.cerevisiae cDNA library (Clontech) (1.8 X 10^5 plaques). The longest cDNA clone was pY34 as shown in Fig.2A. The nucleotide sequence of the clone pY34 and its predicted amino acid sequence are presented in Fig.3. The first possible initiation codon ATG is followed by a segment of 951 bp of the cDNA, forming a single open reading frame that encodes a polypeptide of 317 amino acids with a predicted molecular weight of approximate 35KDa. The in-frame termination codon (TAA) immediately downstream of a Lys-317 is followed by 577 nt of a 3' untranslated region. A search of the EMBL and Swiss-Plot data bases revealed that the cDNA encodes a polypeptide with no apparent sequence similarity as a whole to any previously identified proteins.

The hydropathy plot was obtained by a standard computer-assisted analysis, using the algorithm and hydropathy values of Kyte and Dolittle (101) (Fig.2B). This analysis identified one strongly hydrophobic region. This region contains a stretch of 16 uncharged amino acids extending from Gly-113 to Phe-128, which is followed by three basic amino acids (R-135-K-136-K137). These properties indicate that this region of the 16 amino acids is a membrane-spanning domain, consistent with those observed in the transmembrane segment of many proteins (102). The predicted region recognized by RTM8-2 is located at the sequence from Phe-233 to Asp-248 (Fig.3). The motif search revealed that the pY34 product contains precisely three conserved sites (Gly-83, Gly-117, and Gly-164) known as the addition site for myristic acid (G-{EDKRHPYFW}-x(2)-[STAGCN]-{P}) (103,104). In addition, its product contains a potential N-linked glycosylation site (Asn-60) (105,106,107), and eight potential sites for phosphorylation by protein kinase C ([ST]-x-[RT]) (Ser-6, Thr-67, Ser-97, Ser101, Ser-102, Thr-168, Thr-250, and Ser-266) (108,109).

The homology search of the predicted amino acid sequence indicates a sequence similarity to several identified proteins besides tropomyosins (93,99,100,110) (Fig.4); including the mouse kinesin-like protein (KIF2) (111), the late embryogenesis abundant protein D29 (LEA D29) (112), the Craterostigma Plantaginem dessication-related protein (113), and the Herpesvirus major DNA-binding protein (MBP) (114). The KIF2 protein is one of the kinesin families, which are microtuble-associated motor proteins. The LEA proteins are abundant at the stage of late embryogenesis in higher plant seed embryos, and its function is induced by abscisic acid (leaves and callus) and dessication (leaves). MBP is a single strand DNA-binding protein.

The C-terminal hydrophilic region contains lysine-rich sequences. In addition, this region also contains a C-terminal repeat motif (D-K-A-A-D(E)), which has no apparent sequence similarity to any previously identified motif. In addition a " helix-turn-helix" like structure, identified in a group of DNA binding proteins (115), is indicated in 100 amino acids around the C-terminal 290 amino acid.

As shown in Fig.5, a search through the databases revealed that the sequence of the 3'UTR of Y34 was surprisingly similar to a partial sequence of the human cDNA derived from T lymphoblastoma (EMBL accession number Z15978), and the 3' non-coding region of the Bacillus

circulans 1,3-1,4-B-D-glucanase gene (116). In particular, the 128 nucleotides (from 1036bp to 1163bp) shared a 96.9% similar identity with this sequence. To examine the presence of the sequence, Zoo blotting was carried out on yeast S.cerevisiae (Clontech), a rat (liver and brain), and a human [Hela cells and Placenta (Clontech)], using the pY34 DraI-XbaI fragment as the probe (Fig.6). Several specific bands were detected in yeast, while, in the rat and human DNA, smear bands were detected; the smear bands were detected in the human DNA even under high strigency (63°C) (data not shown). The highly homologous region therefore provides an intriguing clue for examining the function of this protein.

Our approach to search for the homologue of low molecular weight tropomyosin (TM30nm) in S.cerevisiae with the antibody led us to identify an unexpected transmembrane type protein. We named this protein **STRP** (**S**.cerevisiae **T**M30nm **R**elated **P**rotein). The structure indicates the intriguing feature of the trans-membrane protein to have both an actin and DNA modulating function which is regulated through phosphorylation.

References

93. Cayton, L., Reinach, F. C., Chubley, G. M. and MacLeod, A. R. (1988) Organization of the hTMnm gene: Implication for evolution of muscle and non-muscle tropomyosin. J. Mol. Biol. **201**, 507-516.
94. Okamoto-Inoue, M., Taniguchi, S., Sadano, H., Kawano, T., Kimura, G., Gabbiani, G. and Baba, T. (1990) Alteration in expression of smooth muscle α-actin associated with transformation of rat 3Y1 cells. J. Cell Sci. **96**, 631-637.
95. Sambrook, J., Fritsch, E., F. and Maniatis, T. (1989) Molecular Cloning: A Laboratory Mannual, 2nd edn., Cold Spring Harbor Laboratory, Cold Spring Harbor, NY.
96. Sanger, F., Nicklen, S. and Coulson, A. R. (1977) DNA sequencing with chain-terminating inhibitors. Proc. Natl. Acad. USA **74**, 5463-5467.
97. Blin, N. and Stafford, D. W. (1976) A general method for isolation of high molecular weight DNA from eukaryotes. Nucleic Acids Res. **3**, 2303.
98. Gallwitz, D. and Sures, I (1980) Structure of a split yeast gene: complete nucleotide sequence of the actin gene in Sacchromyces cerevisiae. Proc. Natl. Acad. USA **21**, 2546-2550.
99. Liu, H. P. and Bretscher, A. (1989) Disruption of the single tropomyosin gene in yeast results in the disappearance of actin cables from the cytoskeleton. Cell **57**, 233-242.

100. Balasubramanian, M. K., Helfman, D. M. and Hemmingsen, S. M. (1992) A new tropomyosin essential for cytokinesis in the fission yeast S. pombe. Nature **360**, 84-87.

101. Kyte, J. and Doolittle, R. F. (1982) A simple method for displaying the hydropathic character of a protein. J. Mol. Biol. **157**, 105-132.

102. Sabatini, D., Kreibich, G., Morimoto, T. and Adesnik, M. (1982) Mechanisms for the incorporation of proteins in membranes and organelles. J. Cell Biol. **92**, 1-22.

103. Towler, D.A., Eubanks, S.R., Towery, D.S., Adams, S.P. and Glaser, L. (1987) Amino-terminal processing of proteins by N-myristoylation. Substrate specificity of N-myristoyl transferase. J. Biol. Chem. **262**, 1030-1036.

104. Grand, R. J. A. (1989) Acylation of viral and eukaryotic proteins. Biochem. J. **258**, 625-638.

105. Marshall, R. D. (1972) Glycoproteins. Annu. Rev. Biochem. **41**, 673-702.

106. Pless, D. D. and Lennarz, W. J. (1977) Enzymatic conversion of proteins to glycoproteins. Proc. Natl. Acad. Sci. USA. **74**, 134-138.

107. Bause, E. (1983) Structural requirements of N-glycosylation of proteins. Studies with proline peptides as conformational probes. Biochem. J. **209**, 331-336.

108. Woodgett, J. R., Gould, K. L. and Hunter, T. (1986) Substrate specificity of protein kinase C. Use of synthetic peptides corresponding to physiological sites as probes for substrate recognition requirements. **161**, 177-184.

109. Kishimoto, A., Nishiyama, K., Nakanishi, H., Uratsuji, Y., Nomura, H., Takayama, Y. and Nishizuka, Y. (1985) Studies on the phosphorylation of myelin basic protein by protein kinase C and adenosine 3':5'-monophosphate-dependent prtein kinase. J. Biol. Chem. **260**, 12492-12499.

110. Basi, G. S. and Storti, R. V. (1986) Structure and DNA sequence of the tropomyosin I gene from Drosophila melanogaster. J. Biol. Chem. **261**, 817-827.

111. Aizawa, H., Sekine, Y., Takemura, R., Zhang, Z., Nangaku, M. and Hirokawa, N. (1992) Kinesin family in murine central nervous system. J. Cell Biol. **119**, 1287-1296.

112. Baker, J., Steele, C. and Dure, L. (1988) Sequence and characterization of 6 lea protein and their genes from cotton. Plant Mol. Biol. **11**, 277-291.

113. Piatkowski, D., Schneider, K., Saiamini, F. and Bartels, D. (1990) Characterization of five abscisic acid-responsive cDNA clones isolated from the dessication-tolerant plant Craterostigma plantagineum and their relationship to other water-stress genes. Plant Physiol. **94**, 1682-1688.

114. Albrecht, J. C. and Flenckenstein, B. (1990) Structural organization of the conserved gene block of Herpesvirus saimiri coding DNA polymerase, glycoprotein B, and major DNA binding protein. Virology **174**, 277-291.

115. Levine, M. and Hoey, T. (1988) Homeobox proteins as sequence-specific transcription factors. Cell **55**, 537-540.

116. Bueno, A., Vasquez De Aldana, C. R., Correa, J. and Del rey, F. (1990) Nucleotide sequence of a 1,3-1,4-beta-glucanase-encoding gene in Bacillus circulans WL-12. Nucleic Acids Res. **18**, 4248-4248.

Figure legends

Fig.10 Western blotting of yeast and rat tissues using anti-actin and anti-tropomyosin antibodies. The blots of all the protein samples from yeast S.cerevisiae (lane 1), normal rat spleen (lane 2), and normal heart (lane 3) were immunostained with anti-actin antibody (A) (Amersham, UK), anti-tropomyosin antibody (B) (Sigma Chemical Co., St Louis, MO), and anti-TM30nm antibody (RTM8-2) (C). Thirty ug of protein was electrophoresed in each lane. The protein recognized by RTM8-2 was detected in yeast. The positions of the Mr markers are indicated ($X10^3$ dalton) on the right.

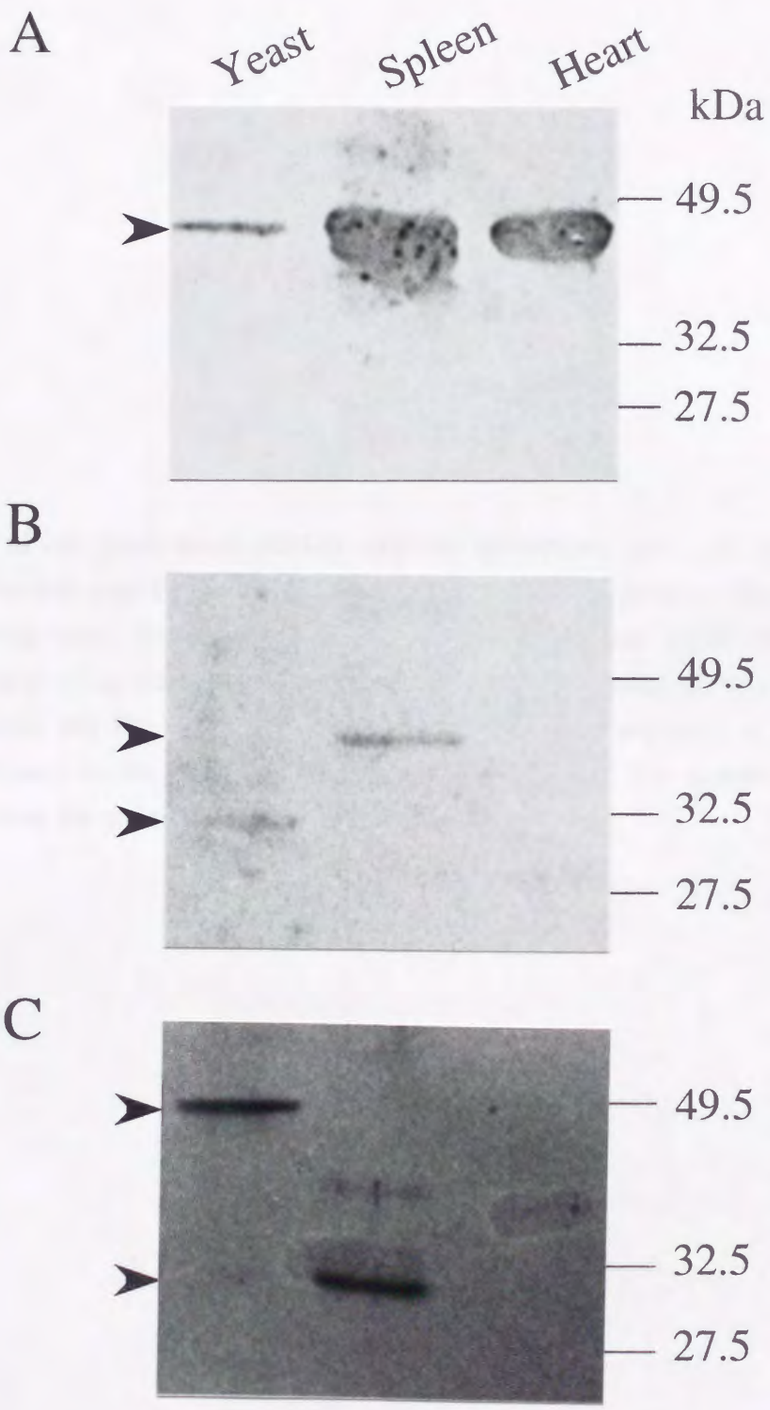
A
Yeast
Spleen
Heart
kDa
49.5
32.5
27.5
B
49.5
32.5
27.5
C
49.5
32.5
27.5

Fig.11 The structure of the yeast novel cDNAs and the hydropathy plot. (A) A schematic representation and restriction map of cDNA (pY34) for a novel yeast protein. The open box represents the open reading frame. The black box indicates the transmembrane region. The cleavage sites for major restriction enzymes are shown. The structure of three overlapping cDNAs (pY5, pY6 and pY29) are also shown. (B) The hydropathy profile of the amino acid sequence of pY34. The hydropathy plot was obtained by the method of Kyte and Doolittle (1982). The numbers under the plot indicate the positions of the amino acid residues in the pY34 product.

A

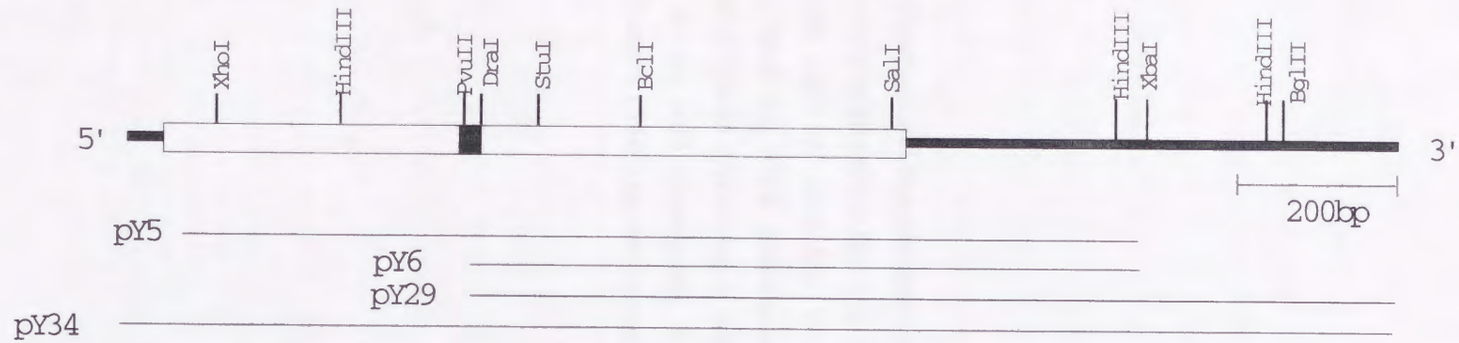
XhoI
HindIII
PvuII
DraI
StuI
BclI
SalI
HindIII
XbaI
HindIII
BglII
5'
3'
200bp
pY5
pY6
pY29
pY34

B

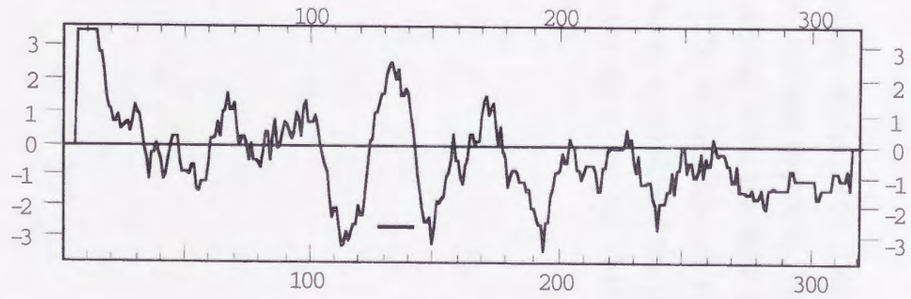
100
200
300
3
2
1
0
-1
-2
-3

Fig.12 The nucleotide sequence and the predicted amino acid sequence of the pY34 cDNA clone. The nucleotides are positively numbered in the 5' to 3' orientation of each lane (top row). The amino acids are numbered to the right of each lane (bottom row), starting with the first in-frame methionine, and ending with the TAA termination codon (*). The transmembrane region is underlined. The predicted N-linked glycosylation site is indicated by an asterisk, and the predicted myristoylation sites are shown with arrowheads. The shadow boxes show the rat TM30nm C-terminal sequence, which seems to be a region recognized by RTM8-2.

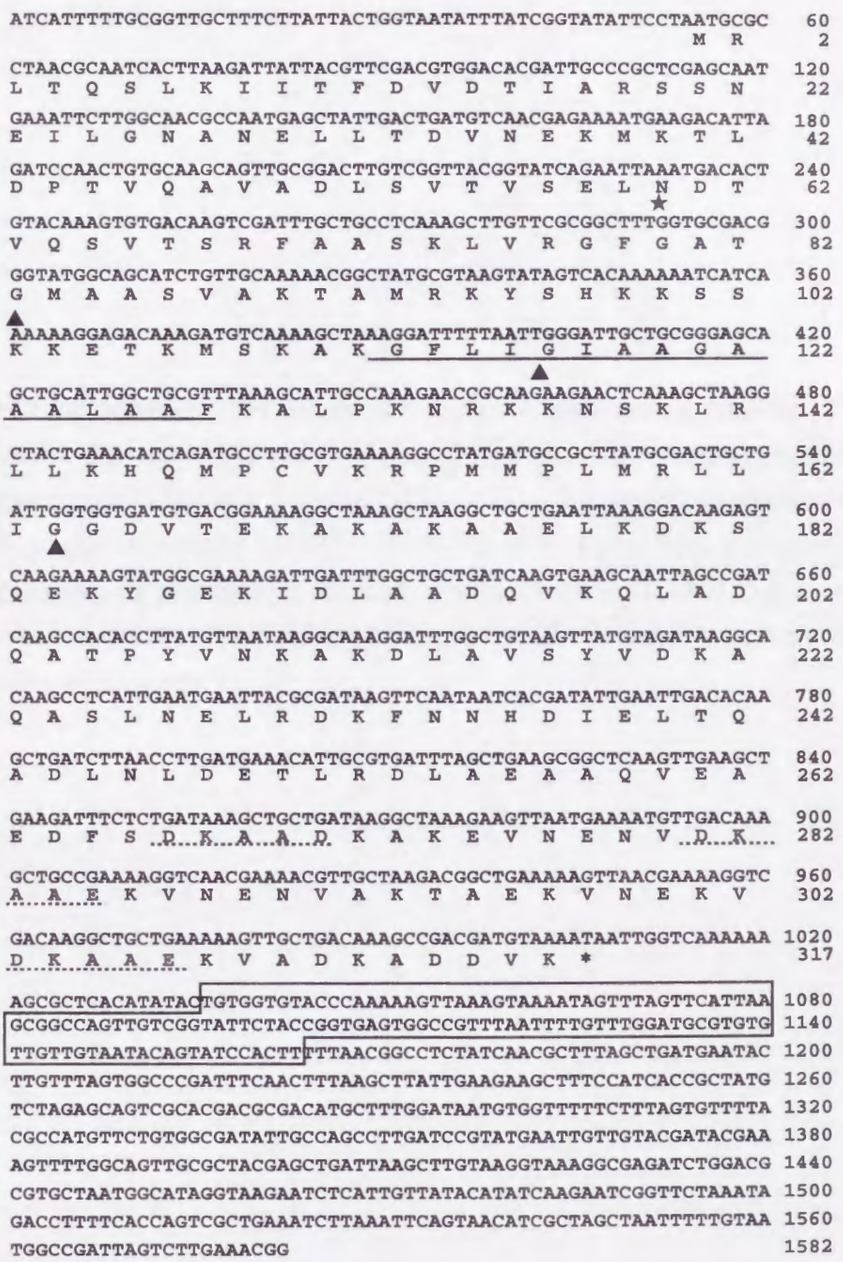

Fig.13 Alignment of the deduced pY34 amino acid sequence with several proteins. The mouse kinesin-like protein KIF2 (Mouse KIF2) (111), Herpesvirus major DNA-binding protein (MDBP) (114), Human tropomyosin TM30nm (HumanTM30) (93), Drosophila tropomyosin TPM1 (DroTPM1) (110), S.pombe tropomyosin cdc8 (yeast cdc8) (100), S.cerevisiae tropomyosin TPM1 (yeastTM1) (99), Craterostigma plantaginem dessication-related protein (DRPF) (113), and the late embryogenesis abundant protein in higher plants (LE29) (112). The residues which are identical to that of STRP are shown as shadows.

```
STRP          1 MRLTQSLKIITFDVDTIARSSNEILGNANELLTDVNEKMKTLDPTVQAVADLSVTVSELN 60
MouseKIF2           665 DVDSYATQLEAILEQKIDILTELRDKVKSFRAALQEEEQAS 705
MDBP        980 VKKNSNLNNLTFEVETIRKNVQNIFEDKDNLNIFDN 1010

STRP         61 DTVQSVTSRFAASKLVRGFGATGMAASVAKTAMRKYSHKKSSKKETKMSKAKGFLIGIAA 120

STRP        121 GAAALAAFKALPKNRKKNSKLRLLKHQMPCVKRPMMPLMRLLIGGDVTEKAKAKAAELKD 180
Yeastcdc8                                                 6 ERINAARAETDE  17
YeastTM1                                                    21 KYEELKE  27

STRP        181 KSQEKYGEKIDLAADQVK-QLADQATPYVNKAKDLAVSYVDKAQASLNELRDKFNNHDIE 239
RatTM30                                              45 AEAEVASLNRRIQLVEEE  62
DroTPM1                              20 DKADTCENQAKD-ANSRADKLNEEVRDLEKKFVQVEID  57
YeastTM1     28 KNKDLEQENVE-KENQIK-SLTVKNQQLEDEIEKLEAGLSDSKQTEQDNV-EK-ENQIKS  83
Yeastcdc8    18 AVARAEAAEAKLKEVELQLSLKEQEYESLSRKSEAAESQLEELEEETKQLRLKADNEDIQ  77
LE29                                    153 KAKDMKDTAYKKTDDVKNAAKGKSSEMRQA 181

STRP        240 LTQADLNLDETLRDLAEAAQVEAEDFSDKAADKAKEV-NENVDKAAEKVNENVAKTAEKV 299
RatTM30      63 LDRAQERLATALQKLEEAEK--AADESERGM-KVIEN-RALKDEEKMELQEIQLKEAKHI 119
DroTPM1      58 LVTAKEQLEKANTELEEKEKLLTATESEVATQN-RKV--QQIEEDLEKSEERSTTAQQKL 114
Yeastcdc8    78 KTEAE-QLSRKV-ELLEEELETNDKLLRETTEKMRQT-DVKAEHFFRRV-QSLERERDDM 133
YeastTM1     84 LTVKNHQLEEEIEKL-EAELAESKQLSE-DSHHLQSN-NDNFSKKNQQLEEDLEESDTKL 140
DRPF                109 ELKDKTQEGAENVREKAMDAGNDA-MEKTRNAGERVADGVSNVGQNV 155
LE29        182 TTEKARELADSAKENANTAYIAAKEKVRDMADRTSEMTNEAQERGARKAEEAKEVVAEKA 242

STRP        299 NEKVDKAAEKVADKADDVK 317
RatTM30     119 AEEADRKYEEVARK 132
DroTPM1     114 LEATQSADE 122
Yeastcdc8   134 EQKLEEMTDKYTKVKAE 150
YeastTM1    141 KETTEK 146
DRPF        155 KENVMGAGEKVKEFAEDVK 173
LE29        243 EGAAEETKKKNEERGESLK 261
```

Fig.14 Zoo blotting of three different organisms using a yeast cloned cDNA as a probe. Representatative Southern blots of genomic DNA from yeast S.cerevisiae, rat, and human were probed with the [^{32}P]CTP labelled pY34 DraI-XbaI fragment under strigency (58°C), as described in the Experimental Procedures. The position of the Mr markers are indicated ($X10^3$ bp).

A

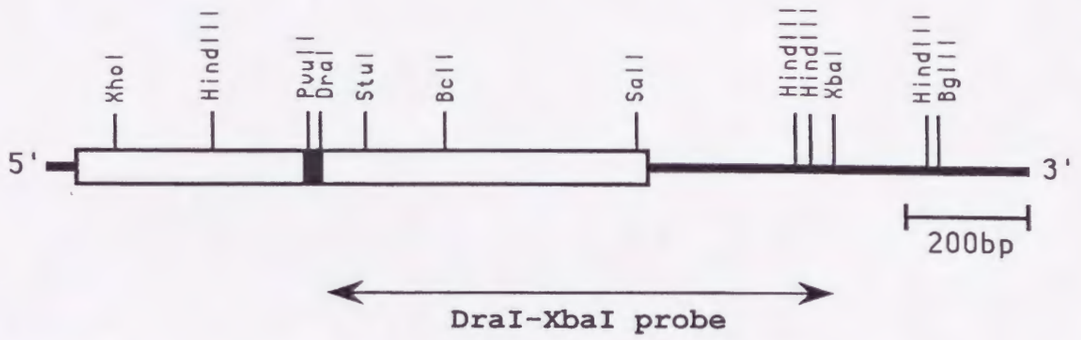
XhoI
HindIII
PvuII
DraI
StuI
BclI
SalI
HindIII
HindIII
XbaI
HindIII
BglII
5'
3'
200bp
DraI-XbaI probe

B

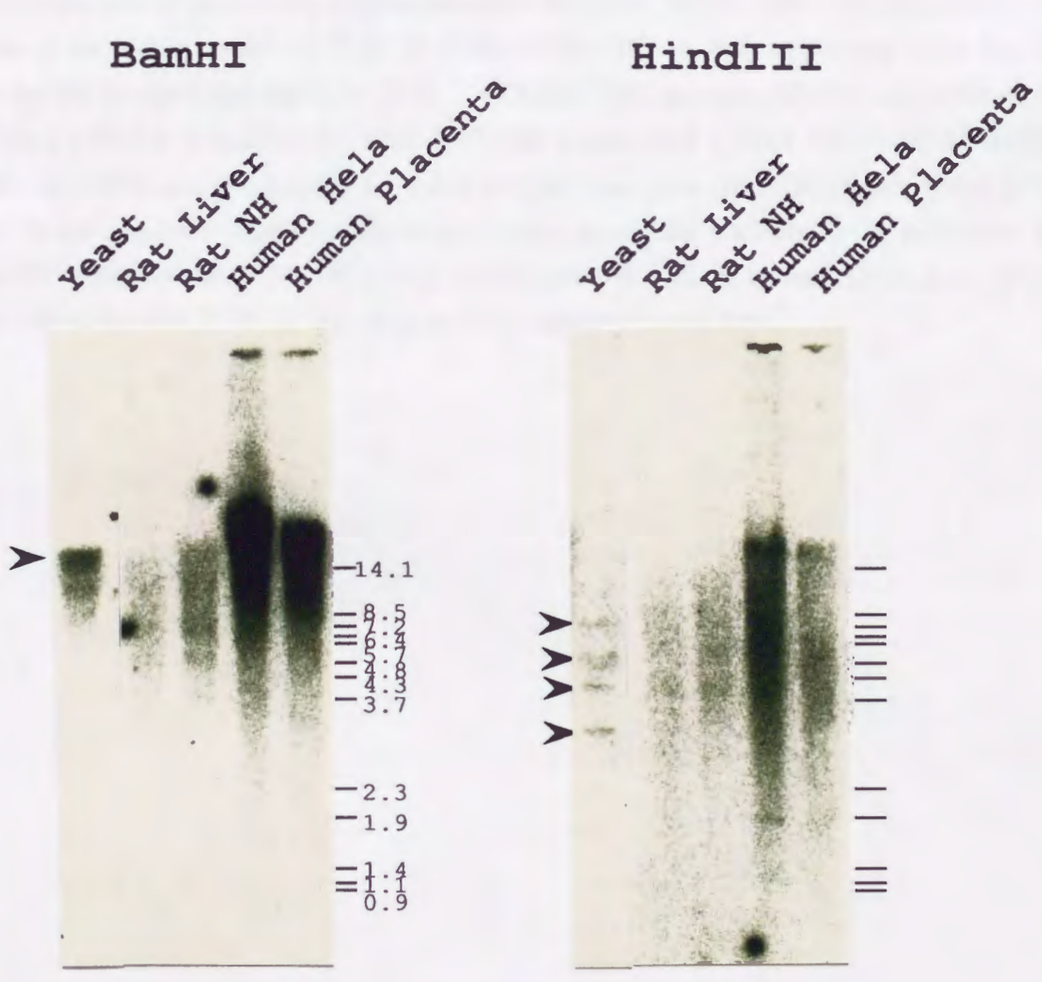
BamHI
HindIII
Yeast
Rat Liver
Rat NH
Human Hela
Human Placenta
Yeast
Rat Liver
Rat NH
Human Hela
Human Placenta
14.1
8.5
7.2
6.4
5.7
4.8
4.3
3.7
2.3
1.9
1.4
1.1
0.9

Fig.15 The alignment of the nucleic acid sequence of the pY34 3'UTR with other sequences. (A) The position of the highly conserved 3' UTR of the pY34 cDNA is indicated by the black box. In this region the site of Age1 endonuclease (5'-A | CCGGT-3') is present. (B) The alignment of the 3' UTR of the pY34 cDNA (nucleotides 1006-1187), the human cDNA clone 54E05 (HSA54EO52) (nucleotides 181-345), and B.circulans 1,3-1,4-B-D-glucanase gene (BCBGC) (nucleotides 1482-1679). The boxed sequence shows the identical residues among the nucleotides. In particular, the nucleotides 1036-1063 of the pY34 cDNA were identical 96.9% with the human cDNA clone 54E05 (EMBL accession number Z15978). This region is indicated by a solid line.

A

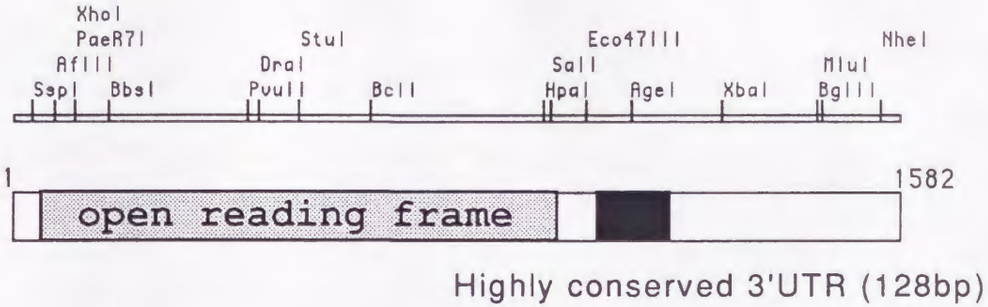
XhoI
PaeR7I
AflII
SspI
BbsI
StuI
DraI
PvuII
BclI
Eco47III
SalI
HpaI
AgeI
XbaI
NheI
MluI
BglII
1
1582
open reading frame
Highly conserved 3'UTR (128bp)

B

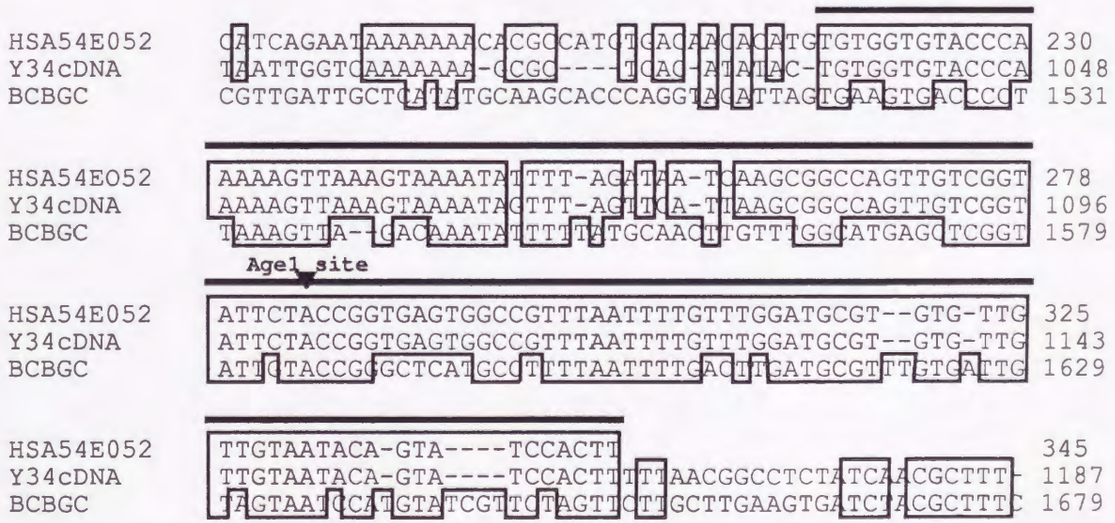
HSA54E052 CATCAGAATAAAAAAACACGCCATGTCACAACACATGTGTGGTGTACCCA 230
Y34cDNA TAATTGGTCAAAAAAA-GCGC----TCAC-ATATAC-TGTGGTGTACCCA 1048
BCBGC CGTTGATTGCTCATATGCAAGCACCCAGGTACATTAGTGAAGTGACCCGT 1531
HSA54E052 AAAAGTTAAAGTAAAATATTTT-AGATAA-TCAAGCGGCCAGTTGTCGGT 278
Y34cDNA AAAAGTTAAAGTAAAATAGTTT-AGTTCA-TTAAGCGGCCAGTTGTCGGT 1096
BCBGC TAAAGTTA--GACAAATATTTTTATGCAACTTGTTTGGCATGAGCTCGGT 1579
AgeI site
HSA54E052 ATTCTACCGGTGAGTGGCCGTTTAATTTTGTTTGGATGCGT--GTG-TTG 325
Y34cDNA ATTCTACCGGTGAGTGGCCGTTTAATTTTGTTTGGATGCGT--GTG-TTG 1143
BCBGC ATTCTACCGGGCTCATGCGTTTTAATTTTGACTTGATGCGTTTGTGATTG 1629
HSA54E052 TTGTAATACA-GTA----TCCACTT 345
Y34cDNA TTGTAATACA-GTA----TCCACTTTTTAACGGCCTCTATCAACGCTTT- 1187
BCBGC TTAGTAATTCATGTATCGTTCTAGTTCTTGCTTGAAGTGATCTACGCTTTC 1679

6. Acknowledgements

I am very grateful to professor Motoya Katsuki and to other members of our labs for advice. I thank Dr. Shun'ichiro Taniguchi for communication of results and for helpful discussions. I also thank Professor Katsuyosi Mihara and Tsuneo Omura for several suggestions.

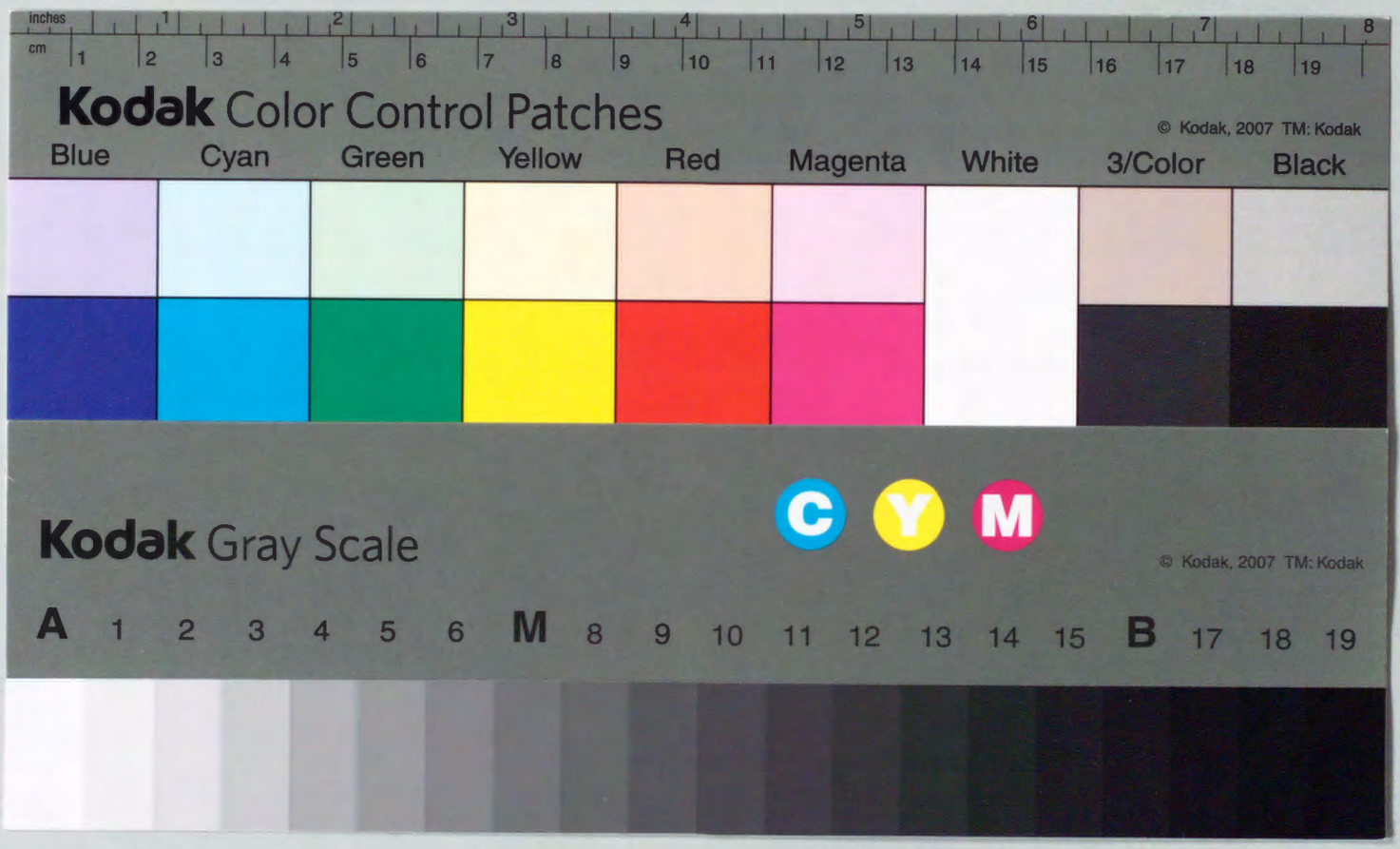
inches
cm
Kodak Color Control Patches
© Kodak, 2007 TM: Kodak
Blue
Cyan
Green
Yellow
Red
Magenta
White
3/Color
Black
Kodak Gray Scale
C
Y
M
© Kodak, 2007 TM: Kodak
A 1 2 3 4 5 6 M 8 9 10 11 12 13 14 15 B 17 18 19